Inorg. Chem. **2002**, *41*, 3396–3409

Synthesis of Heteroleptic Anthryl-Substituted β-Ketoenolates of Rhodium(III) and Iridium(III): Photophysical, Electrochemical, and EPR Study of the Fluorophore–Metal Interaction

Maurizio Carano,[†] Francesca Cicogna,[‡] Julien L. Houben,[§] Giovanni Ingrosso,*[,‡] Fabio Marchetti,[‡] Loïc Mottier,[†] Francesco Paolucci,*[,†] Calogero Pinzino,*[,§] and Sergio Roffia*[,†]

Dipartimento di Chimica "G. Ciamician", Università di Bologna, Via Selmi 2, 40126 Bologna, Italy, Dipartimento di Chimica e Chimica Industriale, Università di Pisa, Via Risorgimento 35, 56126 Pisa, Italy, and Istituto per i Processi Chimico-Fisici del CNR, Area della Ricerca di Pisa, Via G. Moruzzi 1, 56124 Pisa, Italy

Received July 2, 2001

The anthryl-substituted rhodium(III) and iridium(III) heteroleptic β-ketoenolato derivatives of general formula [M(acac)$_2$(anCOacac)] [acac = pentane-2,4-dionate; anCOacac = 3-(9-anthroyl)pentane-2,4-dionate], **3** (M = Rh) and **4** (M = Ir), and [M(acac)$_2$(anCH$_2$acac)] [anCH$_2$acac = 3-(9-anthrylmethyl)pentane-2,4-dionate], **5** (M = Rh) and **6** (M = Ir), were prepared by reacting the corresponding tris(pentane-2,4-dionate)metal complexes, [M(acac)$_3$], with 9-anthroyl chloride and 9-chloromethylanthracene, respectively, under Friedel–Crafts conditions. **3**–**6** were characterized by elemental analysis, ion spray mass spectrometry (IS-MS), ^{1}H NMR, and UV–vis spectroscopy. The structure of **3** was also elucidated by single-crystal X-ray analysis. When excited at 365 nm, **3**–**6** result to be poorly luminescent compounds; while the free diketone, i.e., 3-(9-anthrylmethyl)pentane-2,4-dione **1**, whose structure was established also by single-crystal X-ray analysis, results to be a strongly light emitting molecule. The study of the electrochemical behavior of **3**–**6** as well as of the corresponding tris-acetylacetonates of rhodium(III) and iridium(III) allows a satisfactory interpretation of their electrode process mechanism, and gives information about the location of the redox sites along with the thermodynamic and kinetic characterization of the corresponding redox processes. All data are in agreement with the hypothesis that the quenching of the anthracene fluorescence, observed for compounds **3**–**6**, can be due to an intramolecular electron transfer process between the anthryl moiety and the metal–β-ketoenolato component. Moreover, a study was carried out of the redox behavior of the dyads **3**–**6** under chemical activation. The one-electron oxidation of compounds **3**–**6** by thallium(III) trifluoroacetate leads to the formation of the corresponding cation radicals, **3**$^+$–**6**$^+$, whose highly resolved X-band EPR spectra were fully interpreted by computer simulation as well as by semiempirical and DFT calculations of spin density distribution.

Introduction

The transition metal−β-ketoenolato system can easily undergo one-electron reduction[1] or one-electron oxidation[2] thus giving rise to relatively stable radical species which can be detected and characterized by EPR spectroscopy:

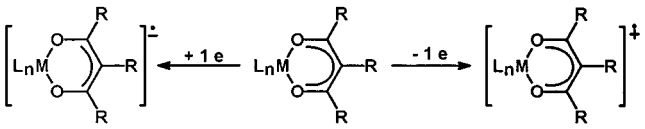

The unpaired electron spin delocalization varies markedly within these radicals and may be ligand- or metal-centered or may interest the whole complex, depending on the structure of the β-ketoenolato ligand. Thus, owing to its electron donor−acceptor properties, the β-ketoenolate−metal moiety appears interesting for projecting new molecular entities in which it is connected to a luminescent fragment. It is expected that the β-ketoenolato−metal system can

* To whom correspondence should be addressed. E-mail: vanni@dcci.unipi.it (G.I.); paolucci@ciam.unibo.it (F.P.); rino@indigo.icqem.pi.cnr.it (C.P.); roffia@ciam.unibo.it (S.R.).
† Università di Bologna.
‡ Università di Pisa.
§ Istituto per i Processi Chimico-Fisici del CNR, Area della Ricerca di Pisa.

(1) Kwan, C. L.; Kochi, J. K. *J. Am. Chem. Soc.* **1976**, *98*, 4903.

10.1021/ic010698x CCC: $22.00
Published on Web 06/04/2002

behave as a unit capable of modifying the physical properties characteristic of the luminescent fragment (light-emitting properties, charge transfer, redox properties, etc.). In other words, the fluorophore could behave as an *antenna* which can harvest light and channel energy to the metal-carrying subunit which results to be electronically modified. Therefore, we were attracted by the idea of synthesizing new transition metal β-ketoenolato derivatives in which at least one of the ligands is linked to a fluorophore through a spacer

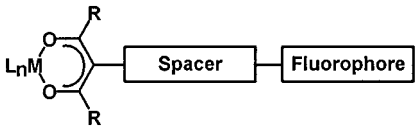

and to state if and how the active sites, i.e., the metal−β-ketoenolato system and the fluorophore, communicate under those conditions (chemical, photochemical, and electrochemical) which can induce the intramolecular transmission of electronic effects.

Research in this field allows scientists to become more familiar with the factors regulating intramolecular energy and electron transfer processes and then to develop new materials with novel characteristics (molecular devices, photoswitches, nonlinear optics, etc.) suitable for use in the field of electronics and telecommunications.[3]

A number of ligands carrying a fluorophore as well as their metal derivatives have been reported,[3c] including several β-diketones containing an efficient light-emitting fragment at position 1 or 3 of the 1,3-propanedione skeleton.[4] The literature documents the preparation of various metal derivatives of these diketones, including aluminum(III),[5] gallium(III),[6] indium(III),[7] zirconium(IV),[8] iron(III),[9] ruthenium(III),[10] and copper(II).[11] Anyway, the luminescence properties of these complexes were not explored. Instead, great attention has been devoted to the study of the sharp emission in the visible and infrared regions exhibited by rare earth anthryl-substituted β-ketoenolates,[12] and more recently it has been shown that various naphthyl-substituted β-ketoenolates of boron exhibit high fluorescence quantum yields.[13]

To our knowledge, only two β-ketoenols carrying an anthracenic moiety at the intercarbonylic carbon atom have been so far reported in the literature, i.e., 3-(9-anthryl)-pentane-2,4-dione, along with its lithium, potassium, beryllium, and palladium(II) derivatives,[14a−c] and a binucleating ligand in which two β-ketoenols are linked to each other by the 1,8-anthracenediyl bridging ligand.[14d] In this connection, it is to be noticed that analogous binucleating ligands have been described but containing 2,7-bis(methylene)naphthalene,[14e] 1,3-bis(methylene)benzene,[14e,f] or 1,4-bis(methylene)benzene as bridging ligands,[14g] along with their copper(II), rhodium(I), and iridium(I) derivatives.

We now report the preparation of new heteroleptic rhodium(III) and iridium(III) β-ketoenolato derivatives hav-

(2) (a) Diversi, P.; Forte, C.; Franceschi, M.; Ingrosso, G.; Lucherini, A.; Petri, M.; Pinzino, C. *J. Chem. Soc., Chem. Commun.* **1992**, 1345. (b) Bruni, M.; Diversi, P.; Ingrosso, G.; Lucherini, A.; Pinzino, C.; Raffaelli, A. *J. Chem. Soc., Dalton Trans.* **1995**, 1035. (c) Bruni, M.; Diversi, P.; Ingrosso, G.; Lucherini, A.; Pinzino, C. *Gazz. Chim. Ital.* **1996**, *126*, 239. (d) Diversi, P.; Ingrosso, G.; Innorta, G.; Lorenzi, R.; Lucherini, A.; Torroni, S. *J. Chem. Soc., Dalton Trans.* **1996**, 2727.

(3) (a) Balzani, V.; Scandola, F. *Supramolecular Photochemistry*; Ellis Horwood: New York, 1991. (b) Bissel, R. A.; De Silva, A. P.; Gunaratne, H. Q. N.; Lynch, P. L.; Maguire, G. E.; McCoy, C. P.; Sandanayake, K. R. A. S. *Top. Curr. Chem.* **1993**, *168*, 223. (c) Ward, M. D. *Chem. Soc. Rev.* **1995**, *24*, 121. (d) Lehn, J. M. *Supramolecular Chemistry. Concepts and Perspectives*; VCH: Weinheim, 1995. (e) Balzani, V.; Juris, A.; Venturi, M.; Campagna, S.; Serroni, S. *Chem. Rev.* **1996**, *96*, 759. (f) Fabbrizzi, L.; Liccarelli, M.; Pallavicini, P.; Perotti, A.; Taglietti, A.; Sacchi, D. *Chem. Eur. J.* **1996**, *2*, 75. (g) De Silva, A. P.; Gunaratne, H. Q. N.; Gunnlaugsson, T.; Huxley, A. J. M.; McCoy, C. P.; Rademacher, J. T.; Rice, T. E. *Chem. Rev.* **1997**, *97*, 1515. (h) Balzani, V.; Campagna, S.; Denti, G.; Juris, A.; Serroni, S.; Venturi, M. *Acc. Chem. Res.* **1998**, *31*, 26. (i) De Cola, L.; Belser, P. *Coord. Chem. Rev.* **1998**, *177*, 301. (j) Prodi, L.; Bolletta, F.; Montalti, M.; Zaccheroni, N. *Eur. J. Inorg. Chem.* **1999**, 455. (k) Collins, G. E.; Choi, L.-S.; Ewing, K. J.; Michelet, V.; Bowen, C. M.; Winkler, J. D. *J. Chem. Soc., Chem. Commun.* **1999**, 321. (l) Fabbrizzi, L.; Gatti, F.; Pallavicini, P.; Zambarbieri, E. *Chem. Eur. J.* **1999**, *5*, 682. (m) Knoblauch, S.; Hartl, F.; Stufkens, D. J.; Hennig, H. *Eur. J. Inorg. Chem.*, **1999**, 303. (n) Fabbrizzi, L.; Licchelli, M.; Parodi, L.; Poggi, A.; Taglietti, A. *Eur. J. Inorg. Chem.* **1999**, 35. (o) Nakashima, K.; Miyamoto, T.; Hashimoto, S. *J. Chem. Soc., Chem. Commun.* **1999**, 213. (p) Pina, F.; Maestri, M.; Balzani, V. *Chem. Commun.* **1999**, 107.

(4) (a) Evans, D. F. *J. Chem. Soc.* **1961**, 1987. Reid, J. C.; Calvin, M. *J. Am. Chem. Soc.* **1950**, *72*, 2948. (b) Veierov, D.; Bercovici, T.; Fischer, E.; Mazur, Y.; Yogev, A. *J. Am. Chem. Soc.* **1973**, *95*, 8173. (c) Veierov, D.; Bercovici, T.; Fischer, E.; Mazur, Y.; Yogev, A. *J. Am. Chem. Soc.* **1977**, *99*, 2723. (d) Veierov, D.; Bercovici, T.; Fischer, E.; Mazur, Y. *J. Org. Chem.* **1978**, *43*, 2006. (e) Veierov, D.; Mazur, Y.; Fischer, E. *J. Chem. Soc., Perkin Trans. 2* **1980**, 1659. (f) Courtot, P.; Le Saint, J.; Pichon, R. *Bull. Soc. Chim. Fr.* **1975**, 2538. (g) Venkataramani, P. S.; Saxema, N. K.; Srinivasan, R.; Ors, J. *J. Org. Chem.* **1976**, *41*, 2784.

(5) Das, M.; Haworth, D. T.; Beery, J. W. *Inorg. Chim. Acta* **1981**, *49*, 17.

(6) Haworth, D. T.; Beery, J. W. *Polyhedron* **1982**, *1*, 9.

(7) (a) Tanner, G. M.; Tuck, D. G.; Wells, E. J. *Can. J. Chem.* **1972**, *50*, 3950. (b) Bowden, K.; Tanner, G. M.; Tuck, D. G. *Can. J. Chem.* **1972**, *50*, 2622.

(8) Das, M.; Beery, J. W.; Haworth, D. T. *Synth. React. Inorg. Met.-Org. Chem.* **1982**, *12*, 671.

(9) (a) Adimado, A. A.; Patel, K. S. *J. Coord. Chem.* **1983**, *13*, 79. (b) Grobelny, R.; Glowiak, T.; Olejnik, Z.; Jezowska-Trzebiatowska, B. *Rocz. Chem.* **1975**, *49*, 477. (c) Grobelny, R.; Jezowska-Trzebiatowska, B.; Wojciechowski, W. *Bull. Acad. Pol. Sci., Ser. Sci. Chim.* **1969**, *17*, 285.

(10) Grobelny, R.; Jezowska-Trzebiatowska, B. *Therm. Anal., Proc. Int. Conf., 4th* **1975**, *2*, 325.

(11) Reichert, C.; Westmore, J. B. *Can. J. Chem.* **1970**, *48*, 3213.

(12) (a) Bauer, H.; Blanc, J.; Ross, D. L. *J. Am. Chem. Soc.* **1964**, *86*, 5125. (b) Filipescu, N.; Mushrush, G. W.; Hurt, C. R.; McAvoy, N. *Nature* **1966**, *212*, 960. (c) Charles, R.; Riedel, E. P. *J. Inorg. Nucl. Chem.* **1967**, *29*, 715. (d) Sato, S.; Wada, M.; Seki, T. *Jpn. J. Appl. Phys.* **1968**, *7*, 7. (e) Tanaka, M.; Yamaguchi, G.; Shiokawa, J.; Yamanaka, C. *Bull. Chem. Soc. Jpn.* **1970**, *43*, 549. (f) Sato, S.; Wada, M. *Bull. Chem. Soc. Jpn.* **1970**, *43*, 1955. (g) Suzuki, M.; Matsui, M.; Shigematsu, T.; Matsuo, Y.; Nagai, T. *Bull. Inst. Chem. Res., Kyoto Univ.* **1980**, *52*, 279. (h) Huang, G.; Hiraki, K.; Nishikawa, Y. *Nippon Kagaku Zaishi* **1981**, 66. (i) Chen, J.; Huang, C. Wan, C.; Xu, G. Sun, J.; Tang, Y. *Wuli Huaxue Xuebao* **1988**, *4*, 494. (j) Morin, M.; Bador, R.; Dechaud, H. *Anal. Chim. Acta* **1989**, *219*, 67. (k) Watarai, H.; Ogawa, K.; Suzuki, N. *Anal. Chim. Acta* **1993**, *277*, 73. (l) Uekawa, M.; Miyamoto, Y.; Hikeida, H.; Kaifu, K.; Nakaya, T. *Synth. Met.* **1997**, *91*, 259.

(13) (a) Ilge, H. D.; Birckner, E.; Fassler, D.; Kozmenko, M. V.; Kuzmin, M. G.; Hartmann, H. *J. Photochem.* **1986**, *32*, 177. (b) Koz'menko, M. V.; Korotkikh, O. A. *Khim. Vys. Energ.* **1990**, *24*, 243. (c) Goerlitz, G.; Hartmann, H. *Heteroat. Chem.* **1997**, *8*, 147.

(14) (a) Kuhr, M.; Musso, H. *Angew. Chem.* **1969**, *81*, 150. (b) Bock, B.; Flatau, K.; Junge, H.; Kuhr, M.; Musso, H. *Angew. Chem., Int. Ed. Engl.* **1971**, *10*, 225. (c) Ismail, M. T. *Bull. Chim. Soc. Fr.* **1987**, *3*, 438. (d) Benites, M. R.; Fronczek, F. R.; Hammer, R. P.; Maverick, A. W. *Inorg. Chem.* **1997**, *36*, 5826. (e) Maverick, A. W.; Buckingham, S. C.; Yao, Q.; Bradbury, J. R.; Stanley, G. G. *J. Am. Chem. Soc.* **1986**, *108*, 7430. (f) Maverick, A. W.; Klavetter, F. E. *Inorg. Chem.* **1984**, *23*, 4130. (g) Whitmore, B. C.; Eisemberg, R. *Inorg. Chem.* **1984**, *23*, 1679.

ing the anthracene fluorophore linked to the intercarbonylic carbon atom of the β-diketonate skeleton through a spacer, and the study of their photophysical and electrochemical properties, along with the EPR study of their one-electron-oxidation products. Brief reports on preliminary results of this study have already been communicated.[15a,b]

This study is a part of a wide research program aimed to state if and how different metal-containing subunits can interact with the anthracene fluorophore. In particular, studies dealing with some anthracene-functionalized cyclopentadienyl derivatives of rhodium(I) and iridium(I) having the following structures have been already published:[15c,d]

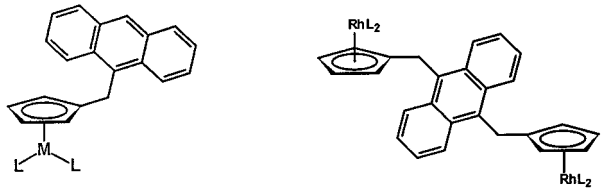

M = Rh or Ir

Experimental Section

Methods and Materials. All solvents were dried and distilled prior to use following standard procedures. Microanalyses were performed by the Laboratorio di Microanalisi, Facoltà di Farmacia, Università di Pisa. Melting or decomposition points were determined by a MEL-TEMP II (Aldrich) apparatus. ^{1}H NMR spectra were run at 200 MHz on a Varian Gemini 200 instrument. Ion spray mass spectra (IS-MS) were performed on a Perkin-Elmer Sciex API III *plus* triple quadrupole mass spectrometer (Sciex Co., Thornhill, Ontario, Canada) equipped with an API ion source and an ion spray interface. The spectra were obtained under the following experimental conditions: ion spray voltage, 5.5 kV; orifice voltage, 35 or 60 V. The samples were dissolved in methanol (ca. 10 mM). Electron ionization mass spectra (EI-MS) were obtained with a VG Analytical 7070E apparatus. UV−visible and fluorescence emission spectra were measured in dichloromethane, as already reported.[15c,d] The electrochemical instrumentation used and the procedure for electrochemical measurements have been already described in detail elsewhere.[15d] For the electrochemical experiments, the solvent was distilled into the electrochemical cell prior to use, using a trap-to-trap procedure.[16] The CV simulations were performed by the DgiSim 3.0 software by Bioanalytical System Inc., and by the Antigona software developed by one of us (L.M.), www.ciam.-unibo.it/electrochem.html. The X-band EPR spectra were obtained, according to published procedures,[2,15d] by a Varian E112 spectrometer, the temperature being controlled by an OXFORD EPR 900 cryostat.[17,18] 9-Anthroyl chloride was prepared as reported.[19] Tris(pentane-2,4-dionate)iridium(III) (Strem Chemicals), tris(pentane-2,4-dionate)rhodium(III) (Aldrich), tris(pentane-2,4-dionate)-cobalt(III) (Aldrich), and 9-chloromethylanthracene (Aldrich) were used as received. K_2CO_3 was dried at 110 °C for 5 h and stored at room temperature under a pure dinitrogen atmosphere before use. Tetrabutylammonium hexafluorophosphate (TBAH, puriss. from Fluka) was used as supporting electrolyte as received. Tris-(trifluoroacetate)thallium(III) (Aldrich) was used as received *[CAUTION: Owing to the toxicity of the thallium derivatives, this compound must be handled with care]*.

Preparation of 3-(9-Anthrylmethyl)pentane-2,4-dione 1. A mixture of 9-chloromethylanthracene (304 mg, 1.34 mmol), anhydrous acetone (2 mL), K_2CO_3 (92.6 mg, 0.67 mmol), and pentane-2,4-dione (130 ìl, 1.34 mmol) was stirred for 12 h at the reflux temperature. Afterward, the mixture was filtered and the resulting solid was washed with acetone. The acetone extracts were collected and dried under reduced pressure (17 mmHg). The crude product so obtained was purified by column (internal diameter, 25 mm; length, 500 mm) chromatography on silica gel 60 (230−400 mesh) (Merck), using dichloromethane as eluant; 279 mg of **1** (72% yield) was obtained as a microcrystalline solid. Mp: 97.5° C.

Anal. Calcd for $C_{20}H_{18}O_2$: C, 82.7; H, 6.3. Found: C, 82.7; H, 6.2.

EI-MS, *m*/*e* (rel int %): 290 (M^+, 15%), 247 ($[M - CH_3CO]^+$, 10), 191 ($[M - CH_3COCHCOCH_3]^+$, 40), 84 (80), 49 (100).

^{1}H NMR ($CDCl_3$), δ (ppm): 1.94 (s, 6 H); 4.17 (m, 3 H); 7.49 (m, 4 H); 8.00 (dd [J = 9.2 Hz; J = 1.66 Hz], 2 H); 8.12 (d [J = 8.8 Hz], 2 H); 8.36 (s, 1 H).

^{1}H NMR (C_6D_6), δ (ppm): 1.16 (s, 6 H); 3.98 (t [J = 6.8 Hz], 1 H); 4.17 (d [J = 6.7 Hz], 2 H); 7.31 (m, 4 H); 7.84 (dd [J = 8.0 Hz; J = 1.5 Hz], 2 H); 8.18 (d [J = 7.4 Hz], 2 H); 8.25 (s, 1 H).

Preparation of [3-(9-Anthroyl)pentane-2,4-dionate]bis(pentane-2,4-dionate)rhodium(III) 3. A solution of tris(pentane-2,4-dionate)rhodium(III) (112 mg, 0.28 mmol) in 1,2-dichloroethane (10 mL) was added at once to a mixture of anthroyl chloride (810 mg, 3.36 mmol), 1,2-dichloroethane (10 mL), and anhydrous $AlCl_3$ (224 mg, 1.67 mmol) at −10 °C, under a pure dinitrogen atmosphere. The reaction mixture was stirred at a temperature ranging from −10° to −5° C for 1 h, and then was treated with cold 10% HCl (40 mL), while being stirred. The aqueous phase was extracted twice with dichloromethane (20 mL). The dichloromethane extracts and the organic phase were collected, washed with water (20 mL), and dried over anhydrous K_2CO_3. The solution was then dried under reduced pressure (17 mmHg). The resulting solid residue was subdivided into ca. 300 mg portions. Each portion was dissolved into dichloromethane (2 mL), and the resulting solution was passed through a column (internal diameter, 5 mm; length, 30 mm) of alumina (aluminum oxide 90, 70−230 mesh, Merck), using dichloromethane as eluant. The first yellow band eluted was collected and dried under reduced pressure (17 mmHg). The microcrystalline solid which resulted was further subdivided into 150 mg portions and each portion was further purified by column (internal diameter, 10 mm; length, 500 mm) chromatography on silica gel 60 (230−400 mesh) (Merck), using dichloromethane as eluant. The first yellow band eluted was discarded. The column was then fed with a dichloromethane/ethyl acetate mixture (9.5/0.5, v/v) which made a second yellow band to be eluted from which **3** was obtained in a pure form. Finally, from the third yellow band eluted, unreacted tris(pentane-2,4-dionate)rhodium-(III) was obtained; 19 mg of **3** (11% yield) was obtained as a yellow microcrystalline solid.

Anal. Calcd for $C_{30}H_{29}O_7Rh$: C, 59.6; H, 4.8. Found: C, 59.5; H, 4.8.

(15) (a) Carano, M.; Cicogna, F.; Houben, J. L.; Ingrosso, G.; Mottier, L.; Paolucci, F.; Pinzino, C.; Roffia, S. 50th ISE Meeting, Pavia, Italy, Sept 5−10, 1999, Abstracts p 888. (b) Cicogna, F.; Houben, J. L.; Ingrosso, G.; Pinzino, C.; Sprugnoli, E. Trends in Transition Metal Chemistry: Towards the Third Millennium, Pisa, Italy, Feb 25−27, 2000, Abstracts p 62. (c) Cicogna, F.; Colonna, M.; Houben, J. L.; Ingrosso, G.; Marchetti, F. *J. Organomet. Chem.* **2000**, *593*−*594*, 251. (d) Carano, M.; Careri, M.; Cicogna, F.; D'Ambra, I.; Houben, J. L.; Ingrosso, G.; Marcaccio, M.; Paolucci, F.; Pinzino, C.; Roffia, S. *Organometallics* **2001**, *20*, 3478.
(16) Carano, M.; Ceroni, P.; Mottier, L.; Paolucci, F.; Roffia, S. *J. Electrochem. Soc.* **1999**, *146*, 3357.
(17) Ambrosetti, R.; Ricci, D. *Rev. Sci. Instrum.* **1991**, *62*, 2281.
(18) EPR-ENDOR, ICQEM-CNR Rome, Italy, Copyright 1992−2000.
(19) Goeckner, N. A.; Snyder, H. R. *J. Org. Chem.* **1973**, *38*, 481.

IS-MS, *m/e*: 605, $[M + H]^+$; 627, $[M + Na]^+$; 643, $[M + K]^+$. ^{1}H NMR ($CDCl_3$), δ (ppm): 2.14 (s, 6 H, CH_3), 2.15 (s, 6 H, CH_3), 2.22 (s, 6 H, CH_3), 5.50 (s, 2 H, CH), 7.45 (m, 4 H, anthryl), 8.00 (m, 2 H, anthryl), 8.20 (m, 2 H, anthryl), 8.50 (s, 1 H, anthryl).

Preparation of [3-(9-Anthroyl)pentane-2,4-dionate]bis(pentane-2,4-dionate)iridium(III) 4. This preparation was carried out exactly as reported above for the preparation of **3**. Starting from 147 mg of tris(pentane-2,4-dionate)iridium (0.36 mmol), 32 mg of **4** (12% yield) was obtained as a yellow microcrystalline solid.

Anal. Calcd for $C_{30}H_{29}O_7Ir$: C, 51.9; H, 4.2. Found: C, 51.8; H, 4.3.

IS-MS, *m/e*: 695 $[M\{^{193}Ir\} + H)]^+$; 693 $[M\{^{191}Ir\} + H]^+$; 717 $[M\{^{193}Ir\} + Na]^+$; 715 $[M\{^{191}Ir\} + Na]^+$; 733 $[M\{^{193}Ir\} + K]^+$; 731 $[M\{^{191}Ir\} + K]^+$.

^{1}H NMR ($CDCl_3$), δ (ppm): 1.97 (s, 6 H, CH_3), 2.00 (s, 6 H, CH_3), 2.07 (s, 6 H, CH_3), 5.49 (s, 2 H, CH), 7.42 (m, 4 H, anthryl), 8.00 (m, 2 H, anthryl), 8.22 (m, 2 H, anthryl), 8.50 (s, 1 H, anthryl).

Preparation of [3-(9-Anthrylmethyl)pentane-2,4-dionate]bis-(pentane-2,4-dionate)rhodium(III) 5. A solution of tris(pentane-2,4-dionate)rhodium(III) (147 mg, 0.36 mmol) in 1,2-dichloroethane (8 mL) was added at once to a mixture of anhydrous $AlCl_3$ (294.4 mg, 2.2 mmol), 9-chloromethylanthracene (1 g, 4.4 mmol), and 1,2-dichloroethane (20 mL) at −30 °C, under a pure dinitrogen atmosphere. The reaction mixture was stirred at a temperature ranging from −30° to −25° C for 1 h, and then was treated with cold (ca. 0° C) 10% HCl (40 mL), while being stirred. After ca. 30 min, the aqueous phase was separated and extracted with dichloromethane (2 × 20 mL). The dichloromethane extracts and the organic phase were collected, washed with water, and dried over anhydrous K_2CO_3. The solution was then dried under reduced pressure (17 mmHg). The resulting solid residue was subdivided into ca. 300 mg portions. Each portion was dissolved in dichloromethane (2 mL), and the resulting solution was passed through a column (internal diameter, 10 mm; length, 100 mm) of alumina (aluminum oxide 90, 70−230 mesh, Merck), using dichloromethane as eluant. The yellow band eluted (10 mL) was collected and dried under reduced pressure (17 mmHg). The resulting crude microcrystalline solid was subdivided into ca. 150 mg portions, and each portion was further purified by column (internal diameter, 10 mm; length, 500 mm) chromatography on silica gel 60 (230−400 mesh) (Merck), using dichloromethane as eluant. The first yellow band eluted was discarded. The column was then fed with a dichloromethane/ethyl acetate mixture (9.5/0.5, v/v), which made a second yellow band to be eluted from which **5** was obtained in a pure form. Finally, from the third yellow band eluted, unreacted tris(pentane-2,4-dionate)rhodium(III) was obtained; 47 mg of **5** (22% yield) was obtained as a yellow microcrystalline solid.

Anal. Calcd for $C_{30}H_{31}O_6Rh$: C, 61.0; H, 5.3. Found: C, 60.7; H, 5.3.

IS-MS, *m/e*: 591, $[M + H]^+$; 613, $[M + Na]^+$; 629 $[M + K]^+$. ^{1}H NMR ($CDCl_3$), δ (ppm): 2.09 (s, 6 H, CH_3), 2.11 (s, 6 H, CH_3), 2.13 (s, 6 H, CH_3), 4.66 (d [J = 15 Hz], 1 H, CH_2), 4.90 (d [J = 15 Hz], 1 H, CH_2), 5.44 (s, 2 H, CH), 7.41 (m, 4 H, anthryl), 7.97 (m, 2 H, anthryl), 8.32 (s, 1 H, anthryl); 8.34 (m, 2 H, anthryl).

Preparation of [3-(9-Anthrylmethyl)pentane-2,4-dionate]bis-(pentane-2,4-dionate)iridium(III) 6. This preparation was carried out as reported above for the preparation of **5**. Starting from 150 mg of tris(pentane-2,4-dionate)iridium (0.36 mmol), 78 mg of **6** (32% yield) was obtained as a yellow microcrystalline solid.

Anal. Calcd for $C_{30}H_{31}O_6Ir$: C, 53.0; H, 4.6. Found: C, 52.8; H, 4.6.

IS-MS, *m/e*: 681, $[M\{^{193}Ir\} + H]^+$; 679, $[M\{^{191}Ir\} + H]^+$; 703, $[M\{^{193}Ir\} + Na]^+$; 701, $[M\{^{191}Ir\} + Na]^+$.

Table 1. Crystal Data and Structure Refinement

	1	**3**
empirical formula	$C_{20}H_{18}O_2$	$C_{30}H_{29}O_7Rh$
fw	290.34	604.44
temp, K	293(2)	293(2)
cryst syst, space group	monoclinic, $P2_1/c$ (No. 14)	monoclinic, $P2_1/n$ (No. 14)
unit cell dimens		
a, Å	17.931(4)	14.371(2)
b, Å	5.396(2)	8.762(2)
c, Å	17.239(3)	21.506(3)
β, deg	107.84(1)	100.19(1)
vol, Å^3	1587.8(7)	2665.3(8)
Z	4	4
ρ_{calc}, Mg/m^3	1.215	1.506
μ, mm^{-1}	0.077	0.687
data/restraints/params	1713/0/199	3706/0/343
$R(F_o)$ $[I > 2\sigma(I)]^a$	0.0715	0.0772
R_w (F_o^2) $[I > 2\sigma(I)]$	0.1488	0.1080

^{a} $R(F_o) = \sum||F_o| - |F_c||/\sum|F_o|$; $R_w(F_o^2) = [\sum[w(F_o^2 - F_c^2)^2]/\sum[w(F_o^2)^2]]^{1/2}$; $w = 1/[\sigma^2(F_o^2) + (AQ)^2 + BQ]$, where $Q = [MAX(F_o^2,0) + 2F_c^2]/3$.

^{1}H NMR ($CDCl_3$), δ (ppm): 1.91 (s, 6 H, CH_3), 1.95 (s, 6 H, s, CH_3), 1.98 (s, 6 H, CH_3), 4.74 (d [J = 17 Hz], 1 H, CH_2), 5.01 (d [J = 17 Hz], 1 H, CH_2), 5.43 (s, 2 H, CH), 7.41 (m, 4 H, anthryl), 7.95 (m, 2 H, anthryl), 8.32 (s, 1 H, anthryl); 8.35 (m, 2 H, anthryl).

X-ray Crystallographic Studies. The diffractometric measurements were carried out at room temperature by means of a Siemens P4 diffractometer equipped with graphite-monochromatic Mo Kα radiation (λ = 0.71073 Å). All data were collected using an $\omega/2\theta$ scan mode, and three standard reflections were monitored every 97 measurements for checking the crystal decay and equipment stability. Data reduction was done by the XSCANS program.[20] All refinement cycles were done by full-matrix least-squares procedures based on F^2.

Single crystals of **1** are pale yellow monoclinic tables defined by the forms corresponding to the basal planes and flattened on {0 0 1}. One of them with dimensions 0.50 × 0.29 × 0.06 mm^3 was glued at the end of a glass fiber, and the cell parameters listed in Table 1 were obtained from the setting angles of 24 strong reflections. The upper θ limit of collection was restricted to 21° because beyond this value the fraction of observed reflections was very low; 2426 reflections, having $-18 \le h \le 17$, $-1 \le k \le 5$, and $-1 \le l \le 17$, were collected. After correction for Lorentz and polarization effects the equivalent reflections were merged, giving a set of 1713 independent reflections ($R_{int} = [\sum|F_o^2 - F_{o\,mean}^2|/\sum(F_o^2)] = 0.059$). The structure solution was obtained by means of direct methods by using the TREF procedure contained in the SHELXTL package.[21] The hydrogen atoms were introduced in calculated positions and allowed to ride on the connected carbon atoms. The final refinement cycle gave the reliability factors listed in Table 1.

A fragment with dimensions 0.22 × 0.06 × 0.06 mm^3 of a yellow needlelike crystal of **3** was glued at the end a glass fiber. The unit cell parameters together with the space group and some structural details are listed in Table 1. The intensity data of 4861 reflections having 2.52° < θ < 23.00° were collected. After correction for Lorentz, polarization, and absorption effects using the ψ-scan method the equivalent reflections were merged, giving a total of 3706 independent reflections (R_{int} = 0,0826). The structure was

(20) XSCANS: *X-ray Single Crystal Analysis System*, rel. 2.1; Siemens Analytical X-ray Instruments Inc.: Madison, WI, 1994.
(21) Sheldrick, G. M. *SHELXTL-Plus*, rel. 5.03; Siemens Analytical X-ray Instruments Inc.: Madison, WI, 1994.

solved by standard Patterson and Fourier methods by means of the SHELX97 program.[22] The hydrogen atoms were placed in calculated positions and allowed to ride on the connected heavy atoms. The final refinement cycles gave the reliability factors listed in Table 1.

Results and Discussion

Preparation of Anthryl-Substituted β-Ketoenolates of Rhodium(III) and Iridium(III). Transition metal β-ketoenolates can be synthesized in different ways, including (i) the reaction of β-diketones with metal salts;[23] (ii) the reaction of metal (main groups) β-ketoenolates with transition metal salts;[24] (iii) the thermally induced ligand-exchange reaction of a transition metal β-ketoenolate with another β-diketone;[25] and (iv) the functionalization of transition metal β-ketoenolates by electrophilic substitution of the intercarbonylic hydrogen atom.[26] Since we were interested in the synthesis of transition metal β-ketoenolates carrying a fluorophoric fragment at the intercarbonylic carbon atom, our first efforts were directed toward the preparation of a simple anthryl-substituted β-diketone, i.e., 3-(9-anthrylmethyl)pentane-2,4-dione **1**, which, to our knowledge, has yet not been described in the literature.

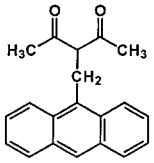

1

Thus, **1** was successfully synthesized by reacting bis(pentane-2,4-dionate)cobalt(II) with 9-chloromethylanthracene or 9-bromomethylanthracene, or by alkylation of pentane-2,4-dione, either in the presence or in the absence of $[CoCl_2(PPh_3)_2]$ as catalyst,[27] the last method leading to higher yields (eq 1).

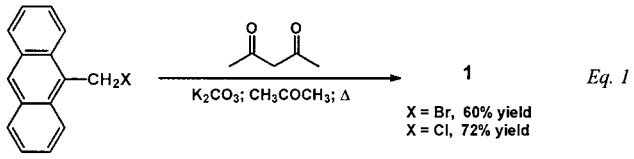

Eq. 1

1 is a crystalline solid which was characterized by elemental analysis, mass spectrometry, ^{1}H NMR, and single-crystal X-ray diffractometry, which reveals that the compound crystallizes exclusively in the β-diketone form, as many other β-diketones do.[28] The molecular structure of **1** is shown in Figure 1. Bond distances and angles are listed in Table 2. The molecule is arranged on four different planes. The first one is that of the 9-anthryl group (carbon atoms C(7)−C(20)), the more deviating atom being C(17) (0.015 Å). The second plane is defined by C(3), C(6), and C(7) atoms. These planes form a dihedral angle of 101.6°. The other two planes, defined by the acetyl groups C(1), C(2), O(1), C(3) and C(4), O(2), C(5), C(3), are approximately perpendicular to each other (87.2°) and make with the anthryl plane the dihedral angles of 46.0° and 106.8°, respectively.

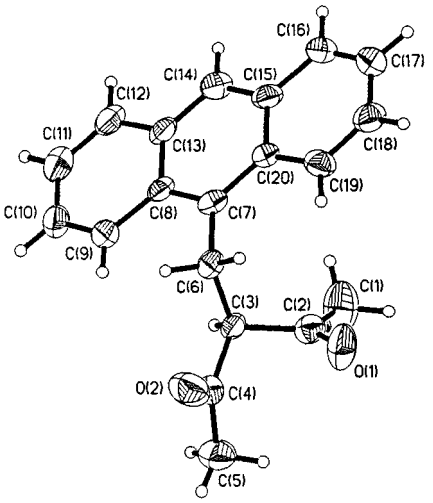

Figure 1. Molecular structure of 3-(9-anthrylmethyl)pentane-2,4-dione **1**; thermal ellipsoids are at 30% probability.

The C═O distances are in keeping, within 3σ, with the mean values observed in $R_2C(sp^2)$═O, 1.210(8).[29] The geometry

(22) Sheldrick, G. M. *SHELX-97, Program for Solution and Refinement of Crystal Structures from Diffraction Data*; Universität Göttingen: Göttingen, Germany, 1997.
(23) Bryant, B. E.; Fernelius, W. C. *Inorg. Synth.* **1957**, *5*, 188.
(24) Kawaguchi, S. *Coord. Chem. Rev.* **1986**, *70*, 51.
(25) (a) Palmer, R. A.; Fay, R. C.; Piper, T. S. *Inorg. Chem.* **1964**, *3*, 875. (b) Collman, J. P.; Sun, J. Y. *Inorg. Chem.* **1965**, *4*, 1273;
(26) Collman, J. P. *Angew. Chem., Int. Ed. Engl.* **1965**, *4*, 132.
(27) (a) Gonzalez, A.; Güell, F.; Marquet, J.; Moreno-Mañas, M. *Tetrahedron Lett.* **1985**, *26*, 3735. (b) Gonzalez, A.; Marquet, J.; Moreno-Mañas, M. *Tetrahedron* **1986**, *42*, 4253. (c) Marquet, J.; Moreno-Mañas, M.; Pacheco, P.; Vallibera, A. *Tetrahedron Lett.* **1988**, *29*, 1465. (d) Gonzales, A.; Marquet, J.; Moreno-Mañas, M. *Tetrahedron Lett.* **1988**, *29*, 1469. (e) Lloris, M. E.; Marquet, J.; Moreno-Mañas, M. *Tetrahedron Lett.* **1990**, *31*, 7489. (f) Lloris, M. E.; Gálvez, N.; Marquet, J.; Moreno-Mañas, M. *Tetrahedron* **1991**, *47*, 8031. (g) Moreno-Mañas, M.; Gonzalez, A.; Jaime, C.; Lloris, M. E.; Gálvez, N.; Marquet, J.; Martinez, A.; Siani, A. C.; Vallibera, A.; Hernández-Fuentes, I.; Rey-Stolle, M. F.; Salom, C. *Tetrahedron* **1991**, *47*, 6520. (h) Vallibera, A.; Marquet, J.; Moreno-Mañas, M.; Cayón, E. *Tetrahedron* **1993**, *49*, 6437. (i) Jeffery, J. C.; Kurek, S. S.; McCleverty, J. A.; Psillakis, E.; Richardson, R. M.; Ward, M. D.; Wlodarczyk, A. *J. Chem. Soc., Dalton Trans.* **1994**, 2559.
(28) (a) Tonnesen, H. H.; Karlsen, J.; Mostad, A. *Acta Chem. Scand., Ser. B* **1982**, *36*, 475. (b) Williams, D. E.; Dumke, W. L.; Rundle, R. E. *Acta Crystallogr.* **1962**, *15*, 627. (c) Engebretson, G. R.; Rundle, R. E. *J. Am. Chem. Soc.* **1964**, *86*, 574. (d) Kutschabsky, L.; Argay, G.; Fischer, G. W.; Zimmermann, T. *Z. Chem.* **1984**, *24*, 216. (e) Bailey, N. A.; Fenton, D. E.; Gayda, S. E.; Phillips, C. A. *J. Chem. Soc., Dalton Trans.* **1984**, 2289. (f) Cannon, J. R.; Patrick, V. A.; White, A. H. *Aust. J. Chem.* **1986**, *39*, 1811. (g) Mullica, D. F.; Karban, J. W.; Grossie, D. A. *Acta Crystallogr. C* **1987**, *43*, 601. (h) Fox, J. L.; Chen, C. H.; Luss, H. R. *J. Org. Chem.* **1987**, *52*, 2980. (i) De March, P.; Moreno-Mañas, M.; Roca, J. L.; Germain, G.; Piniella, J. F.; Dideberg, O. *J. Heterocycl. Chem.* **1986**, *23*, 1511. (j) Emsley, J.; Freeman, N. J.; Hursthouse, M. B.; Bates, P. A. *J. Mol. Struct.* **1987**, *161*, 181. (k) Abbott, P. J.; Acheson, R. M.; Procter, G.; Watkin, D. J. *Acta Crystallogr. B* **1978**, *34*, 2165. (l) Cunnigham, B. D. M.; Lowe, P. R.; Threadgill, M. D. *J. Chem. Soc., Perkin Trans. 2* **1989**, 1275. (m) Sans-Lenain, S.; Reynes, A.; Gleizes, A. *Acta Crystallogr. C* **1992**, *48*, 1788. (n) Hamdi, M.; Speziale, V.; Jaud, J. *Z. Crystallogr.* **1994**, *209*, 495. (o) Kataeva, O. N.; Litvinov, I. A.; Naumov, V. A.; Polozov, A. M.; Polezhaeva, N. A. *Zh. Obshch. Khim.* **1990**, *60*, 555. (p) Yu. Antipin, M.; Kalinin, A. E.; Struchkov, Y. T.; Aladzheva, I. M.; Mastryukova, T. A.; Kabach, M. I. *Zh. Strukt. Khim.* **1980**, *21*, 175. (q) Pandolfo, L.; Facchin, G.; Bertani, R.; Ganis, P.; Valle, G. *Angew. Chem., Int. Ed. Engl.* **1994**, *33*, 576. (r) Pandolfo, L.; Bertani, R.; Facchin, G.; Zanotto, L.; Ganis, P.; Valle, G.; Seraglia, R. *Inorg. Chim. Acta* **1995**, *27*, 237. (s) Kopf, J.; Bretzke, C.; Domnin, I. N.; Plotkin, V. N. *Acta Crystallogr. C* **1996**, *52*, 722.
(29) Allen, F. H.; Kennard, O.; Watson, D. G.; Brammer, L.; Orpen, A. G.; Taylor, R. *J. Chem. Soc., Perkin Trans. 2* **1987**, S1.

around C(3) indicates a normal sp^3 coordination as expected for the diketo tautomer.

When **1** is treated with various salts of 8, 9, and 10 group transition metals in alcoholic or aquoalcoholic media under the experimental conditions in which a great number of homo- and heteroleptic β-ketoenolates have been prepared,[30] no reaction takes place, unless a base is present. In this case, **1** is partially or completely transformed into the ketone **2** (eq 2).

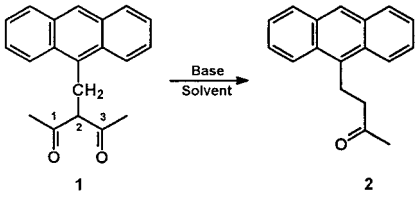

1 **2** *Eq. 2*

The literature documents that several aryl- or alkyl-substituted β-diketones,[31] as well as β-diesters and β-keto esters,[32] can undergo the metal-catalyzed alcoholysis of the C(1)−C(2) bond of the 1,3-propanedione skeleton, thus giving rise to ketones such as **2**. Anyway, in the case of **1** the presence of a base is necessary for such a reaction to take place. Indeed, the ketone **2** is invariably obtained, along with minor amounts of other unidentified products, when **1** is reacted with K_2CO_3, KOH, EtONa, *t*-BuOK, NaH, EtOTl, or metallic sodium, at temperatures ranging from 0° to ca. 40° C, adopting reaction times ranging from 10 min to 18 h. The presence of electron-releasing substituents at the central carbon atom of pentane-2,4-dione causes a marked shift of the keto−enol equilibrium toward the keto form.[24] The equilibrium constant (K = enol/keto) for pentane-2,4-dione is 3.65 (CCl_4, NMR), while that for 3-methyl-pentane-2,4-dione goes to 0.39 (CCl_4, NMR).[33] The ^{1}H NMR spectrum of **1** shows that the enol tautomer is practically nonexistent, both in chloroform and in benzene. In particular, the spectrum in C_6D_6 exhibits a sharp triplet (δ = 3.97 ppm, J = 6.8 Hz) and a sharp doublet (δ = 4.17 ppm, J = 6.7 Hz) due to the intercarbonylic proton and to the methylene protons, respectively, and no other signals attributable to the enolic form. Therefore, one can conclude that the very scarce tendency of **1** to exist in the enolic form prevents its deprotonation, and the base-catalyzed hydrolysis results then to be favored.

Table 2. Bond Lengths (Å) and Angles (deg) for **1**

C(1)−C(2)	1.456(10)	C(9)−C(10)	1.358(9)
C(2)−O(1)	1.186(8)	C(10)−C(11)	1.399(10)
C(2)−C(3)	1.538(9)	C(11)−C(12)	1.358(9)
C(3)−C(4)	1.512(9)	C(12)−C(13)	1.433(10)
C(3)−C(6)	1.534(7)	C(13)−C(14)	1.396(9)
C(4)−O(2)	1.222(9)	C(14)−C(15)	1.395(9)
C(4)−C(5)	1.491(10)	C(15)−C(20)	1.431(9)
C(6)−C(7)	1.508(8)	C(15)−C(16)	1.436(9)
C(7)−C(8)	1.415(8)	C(16)−C(17)	1.341(9)
C(7)−C(20)	1.422(9)	C(17)−C(18)	1.400(10)
C(8)−C(13)	1.430(9)	C(18)−C(19)	1.348(9)
C(8)−C(9)	1.441(8)	C(19)−C(20)	1.427(9)
O(1)−C(2)−C(1)	121.8(8)	C(9)−C(10)−C(11)	121.4(8)
O(1)−C(2)−C(3)	120.2(8)	C(12)−C(11)−C(10)	119.9(8)
C(1)−C(2)−C(3)	118.0(8)	C(11)−C(12)−C(13)	121.6(8)
C(4)−C(3)−C(6)	112.2(6)	C(14)−C(13)−C(8)	120.2(8)
C(4)−C(3)−C(2)	107.0(6)	C(14)−C(13)−C(12)	121.4(8)
C(6)−C(3)−C(2)	110.8(6)	C(8)−C(13)−C(12)	118.4(8)
O(2)−C(4)−C(5)	121.0(9)	C(13)−C(14)−C(15)	120.5(8)
O(2)−C(4)−C(3)	121.0(8)	C(14)−C(15)−C(20)	120.2(7)
C(5)−C(4)−C(3)	117.9(8)	C(14)−C(15)−C(16)	120.5(8)
C(7)−C(6)−C(3)	113.4(5)	C(20)−C(15)−C(16)	119.3(8)
C(8)−C(7)−C(20)	118.9(7)	C(17)−C(16)−C(15)	120.5(8)
C(8)−C(7)−C(6)	119.7(7)	C(16)−C(17)−C(18)	120.4(8)
C(20)−C(7)−C(6)	121.4(7)	C(19)−C(18)−C(17)	121.6(8)
C(7)−C(8)−C(13)	120.2(7)	C(18)−C(19)−C(20)	121.0(7)
C(7)−C(8)−C(9)	122.0(7)	C(7)−C(20)−C(19)	122.8(7)
C(13)−C(8)−C(9)	117.8(7)	C(7)−C(20)−C(15)	120.0(7)
C(10)−C(9)−C(8)	120.9(8)	C(19)−C(20)−C(15)	117.1(7)

Since our attempts to synthesize anthryl-functionalized β-ketoenolato derivatives of transition metals starting from **1** failed, we turned our attention to the possibility of replacing the central hydrogen atom on the pentane-2,4-dionate−metal system by a group carrying the anthracenic chromophore under electrophilic conditions.[26,34] Thus, the tris(pentane-2,4-dionate) derivatives of cobalt(III), rhodium(III), and iridium(III) were reacted with 9-anthroyl chloride in the presence of $AlCl_3$, under the classical Friedel−Crafts conditions.[35] The attempted acylation of cobalt(III) acetylacetonate failed, largely because of the acid-promoted degradation of the starting complex. Instead, the reaction of the rhodium(III) and iridium(III) acetylacetonates led to the monoacylated derivatives **3** and **4**, respectively, of formula [M(acac)$_2$(anCOacac)] (anCOacac = 3-(9-anthroyl)pentane-2,4-dionate) (Scheme 1). Analogously, the $AlCl_3$-promoted reaction of 9-chloromethylanthracene with tris(pentane-2,4-dionate)rhodium(III) and tris(pentane-2,4-dionate)iridium(III) led to the monoalkylated derivatives **5** and **6** of formula [M(acac)$_2$(anCH$_2$acac)] (anCH$_2$acac = 3-(9-anthrylmethyl)pentane-2,4-dionate) (Scheme 1).

It is interesting to emphasize that the Friedel−Crafts acylation and alkylation of rhodium(III) and iridium(III) acetylacetonates both lead to the monosubstituted products and 50−70% recovered starting material, even using a large excess of acylating or alkylating agent. The poor yields obtained (Scheme 1) can be associated with the already

(30) (a) Cervelló, J.; Marquet, J.; Mañas, M. *Synth. Commun.* **1990**, *20*, 1931. (b) Murakami, Y.; Nakamura, K.; Uchida, H.; Kanaoka, Y. *Inorg. Chim. Acta* **1968**, *2*, 133. (c) Addison, A. W.; Graddon, D. P. *Aust. J. Chem.* **1968**, *21*, 1, 2003. (d) Murakami, Y.; Nakamura, K. *Bull. Chem. Soc. Jpn.* **1966**, *39*, 901. (e) Graddon, D. P.; Schultz, R. A. *Aust. J. Chem.* **1965**, *18*, 1731. (f) Arnett, E. M.; Freiser, H.; Mendelsohn, M. A. *J. Am. Chem. Soc*. **1962**, *84*, 2482. (g) Charles, R. G.; Pawlikowski, M. A. *J. Phys. Chem.* **1958**, *62*, 440. (h) Holtzclaw, H. F.; Collman, J. P. *J. Am. Chem. Soc.* **1957**, *79*, 3318. (i) Si, Z.; Jiao, X.; Hu, B. *Synthesis* **1990**, 590. (j) Ribeiro da Silva, M. A. V.; Reis, A. M. M. V. *Bull. Chem. Soc. Jpn.* **1979**, *52*, 3080. (k) Zaugg, H. E.; Schaefer, A. D. *J. Am. Chem. Soc.* **1965**, *87*, 1857. (l) Fackler, J. P.; Cotton, F. A. *J. Am. Chem. Soc.* **1961**, *83*, 3775.
(31) Uehara, K.; Kitamura, F.; Tanaka, M. *Bull. Chem. Soc. Jpn.* **1976**, *49*, 493.
(32) (a) Bickel, C. L. *J. Am. Chem. Soc.* **1945**, *67*, 2204. (b) Hauser, C. R.; Swamer, F. W.; Ringler, B. I. *J. Am. Chem. Soc.* **1948**, *70*, 4023. (c) Pearson, R. G.; Mayerle, E. A. *Bull. Chem. Soc. Jpn.* **1951**, *24*, 926. (d) Pearson, R. G.; Sandy, A. C. *Bull. Chem. Soc. Jpn.* **1951**, *24*, 931. (e) Calmon, J.-P.; Maroni, P. *Bull. Soc. Chim. Fr.* **1968**, 3761.
(33) Allen, G.; Dwek, R. A. *J. Chem. Soc. B* **1966**, 161.
(34) Mehrotra, R. C.; Bohra, R.; Caur, D. P. *Metal β-diketonates and allied derivatives*; Academic Press: London, 1978.
(35) Collman, J. P.; Marshall, L.; Young, W. L., III; Sears, R. T., Jr. *J. Org. Chem.* **1963**, *28*, 1449.

Scheme 1

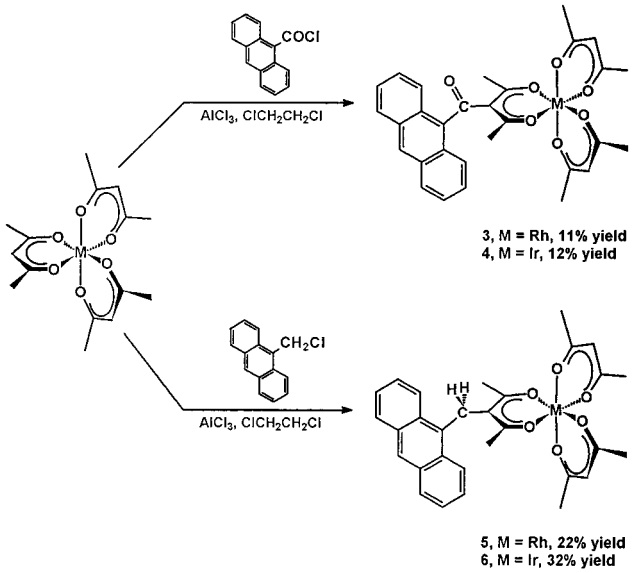

observed relatively scarce reactivity of tris(pentane-2,4-dionate)rhodium(III) toward Friedel−Crafts acylating reagents, if compared with that exhibited by the tris(pentane-2,4-dionate)chromium(III).[35] Moreover, the importance of steric factors in influencing the reaction course cannot be ruled out. In fact, while tris(pentane-2,4-dionate)rhodium(III) can be acetylated to the mono- and disubstituted rhodium chelates (ca. 35% and 11% yield, respectively), its reaction with benzoyl chloride gives only the monobenzoyl compound, in the same yield (11%)[35] that we observed in the synthesis of the monosubstituted complex **3**. To our knowledge no data are reported in the literature concerning the behavior of tris(pentane-2,4-dionate)iridium(III) toward Friedel−Crafts acylating agents. However, it is likely that rhodium and iridium behave quite similarly. The reactions of rhodium and iridium chelates with 9-chloromethylanthracene, under Friedel−Crafts conditions, deserve similar comments, although it is noteworthy that both the monosubstituted rhodium(III) and iridium(III) chelates are now obtained in yields markedly higher (22% and 32%, respectively) than those observed in the acylation reactions.

Complexes **3**−**6** were characterized by elemental analysis, ion spray mass spectrometry (IS-MS), and ^{1}H NMR. **3** was also characterized by single-crystal X-ray diffractometry. The molecular structure of **3** is shown in Figure 2. Bond distances and angles are listed in Table 3. The rhodium coordination is a distorted octahedron and is similar to that observed for tris(pentane-2,4-dionate)rhodium(III)[36] and tris(1,1,1-trifluoropentane-2,4-dionate)rhodium(III).[37]

The distortion is mainly due to the acac bite (O···O 2.93 Å), which is too high for allowing an O−Rh−O angle of 90°. Thus, the O(1)−Rh−O(2) and O(3)−Rh−O(4) angles are 95°. The two resulting rhodadioxacyclohexane rings are almost planar with a maximum deviation of 0.03 Å. On the contrary, the 3-(9-anthroyl)pentane-2,4-dionate ligand is not planar, probably due to a compromise between the delocalization energy, asking for an anthroyl CO coplanar with the acac system, and the hindrance of the methyl groups not allowing such a coplanarity. The noncoplanarity of C(16)−

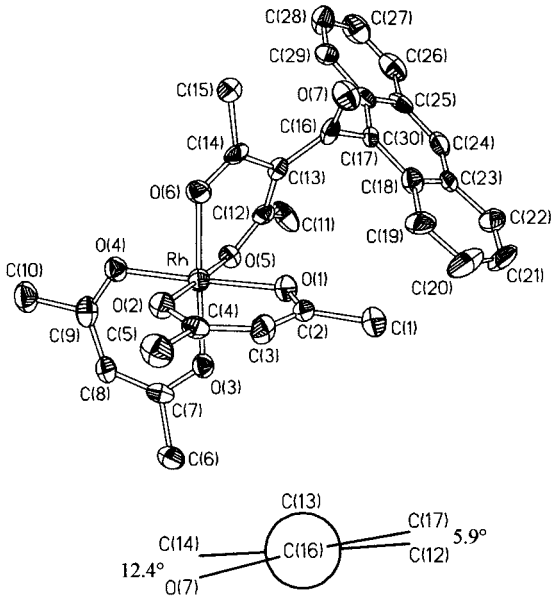

Figure 2. Molecular structure of [3-(9-anthroyl)pentane-2,4-dionate]bis-(pentane-2,4-dionate)rhodium(III) **3** and Newman projection along the C(13)−C(16) bond.

Table 3. Bond Lengths (Å) and Angles (deg) for **3**

Rh−O(3)	1.970(8)	C(2)−C(3)	1.393(16)
Rh−O(6)	1.985(8)	C(3)−C(4)	1.385(15)
Rh−O(2)	1.989(8)	C(4)−C(5)	1.490(15)
Rh−O(4)	1.990(7)	C(6)−C(7)	1.507(16)
Rh−O(1)	1.996(8)	C(7)−C(8)	1.386(16)
Rh−O(5)	1.998(85)	C(8)−C(9)	1.398(18)
O(1)−C(2)	1.263(14)	C(9)−C(10)	1.504(15)
O(2)−C(4)	1.265(13)	C(11)−C(12)	1.509(15)
O(3)−C(7)	1.272(13)	C(12)−C(13)	1.414(16)
O(4)−C(9)	1.270(15)	C(13)−C(14)	1.459(15)
O(5)−C(12)	1.272(13)	C(13)−C(16)	1.473(16)
O(6)−C(14)	1.271(14)	C(14)−C(15)	1.475(16)
O(7)−C(16)	1.225(15)	C(16)−C(17)	1.549(15)
C(1)−C(2)	1.501(14)		
O(3)−Rh−O(6)	177.2(4)	C(4)−C(3)−C(2)	129.6(12)
O(3)−Rh−O(2)	88.1(3)	O(2)−C(4)−C(3)	125.1(12)
O(6)−Rh−O(2)	91.8(3)	O(2)−C(4)−C(5)	114.8(11)
O(3)−Rh−O(4)	94.9(3)	C(3)−C(4)−C(5)	120.1(12)
O(6)−Rh−O(4)	87.8(4)	O(3)−C(7)−C(8)	126.4(12)
O(2)−Rh−O(4)	87.0(3)	O(3)−C(7)−C(6)	115.5(12)
O(3)−Rh−O(1)	86.1(3)	C(8)−C(7)−C(6)	118.1(13)
O(6)−Rh−O(1)	91.2(3)	C(7)−C(8)−C(9)	126.5(13)
O(2)−Rh−O(1)	95.2(4)	O(4)−C(9)−C(8)	126.7(12)
O(4)−Rh−O(1)	177.7(4)	O(4)−C(9)−C(10)	115.9(13)
O(3)−Rh−O(5)	91.8(3)	C(8)−C(9)−C(10)	117.4(14)
O(6)−Rh−O(5)	88.4(3)	O(5)−C(12)−C(13)	126.5(12)
O(2)−Rh−O(5)	177.8(4)	O(5)−C(12)−C(11)	110.3(12)
O(4)−Rh−O(5)	90.9(3)	C(13)−C(12)−C(11)	123.1(11)
O(1)−Rh−O(5)	86.9(3)	C(12)−C(13)−C(14)	118.8(11)
C(2)−O(1)−Rh	122.5(8)	C(12)−C(13)−C(16)	125.9(12)
C(4)−O(2)−Rh	122.3(8)	C(14)−C(13)−C(16)	115.3(12)
C(7)−O(3)−Rh	123.3(8)	O(6)−C(14)−C(13)	124.2(12)
C(9)−O(4)−Rh	122.3(8)	O(6)−C(14)−C(15)	114.5(11)
C(12)−O(5)−Rh	122.2(8)	C(13)−C(14)−C(15)	121.1(12)
C(14)−O(6)−Rh	124.2(8)	O(7)−C(16)−C(13)	122.6(13)
O(1)−C(2)−C(3)	124.8(12)	O(7)−C(16)−C(17)	115.7(12)
O(1)−C(2)−C(1)	115.1(13)	C(13)−C(16)−C(17)	121.6(13)
C(3)−C(2)−C(1)	120.1(13)		

(36) Morrow, J. C.; Parker Junior E. B. *Acta Crystallogr., Sect. B* **1973,** *29*, 1145.
(37) Baidina, I. A.; Stabnikov, P. A.; Igumenov, I. K.; Borisov, S. V. *Koord. Khim.* **1986**, *12*, 404.

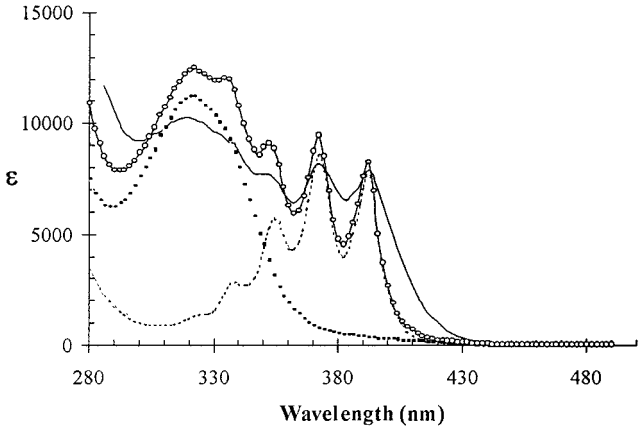

Figure 3. Comparison of the UV−vis spectrum of [Rh(anCOacac)(acac)$_2$] **3** (—) with the sum (−○−) of the UV−vis spectra of 9-acetylanthracene (- - -) and [Rh(acac)$_3$] (■).

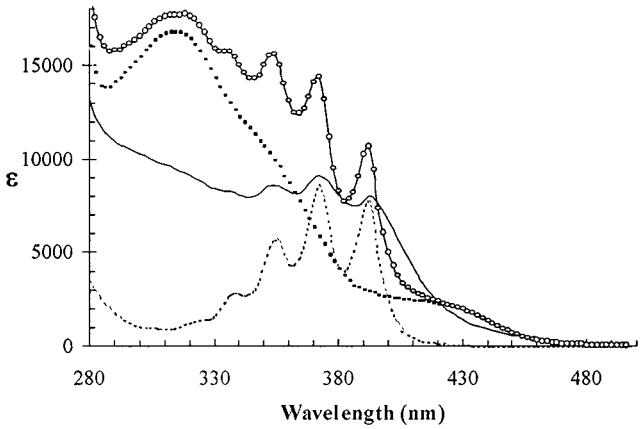

Figure 4. Comparison of the UV−vis spectrum of [Ir(anCOacac)(acac)$_2$] **4** (—) with the sum (−○−) of the UV−vis spectra of 9-acetylanthracene (- - -) and [Ir(acac)$_3$] (■).

O(7) with respect to the C(12)C(13)C(14) plane is illustrated by the Newman-like projection reported in the Figure 2. The 3-anthroylacetyacetonate group has the C(11), C(12), C(13), and O(5) and C(13), C(14), C(15), and O(6) atoms on two different planes making a dihedral angle of 28°, thus approaching O(5) and O(6) atoms (2.78 Å) and reducing the bite of the ligand (O(5)−Rh−O(6) angle = 88°). Moreover, probably due to the ligand distortion and to the hindrance of anthroyl group, a dihedral angle of 152° is observed between the O(5)RhO(6) and C(12)O(5)C(14)O(6) planes. Finally, a dihedral angle of 84° is present between the 9-anthryl plane and the C(13)C(16)O(7)C(17) plane. Values near 90° have been regularly observed in all the known structures of anthroyl derivatives.

Spectroscopic and Photophysical Studies. UV−vis spectral parameters of complexes **3**−**6** along with those of 9-methylanthracene **7**, 3-(9-anthrylmethyl)-pentane-2,4-dione **1**, [Rh(acac)$_3$], and [Ir(acac)$_3$] are reported in Figures 3−6 and in Table 4. The same vibrational progression is observed in all of these compounds, and, as expected,[38] there is a pronounced shift of the maxima positions compared to anthracene upon substitution at position 9. This shift is quite

(38) Jaffé, H. H.; Orchin, M. *Theory and Applications of Ultraviolet Spectroscopy*; John Wiley & Sons: New York, 1966; pp 305−316.

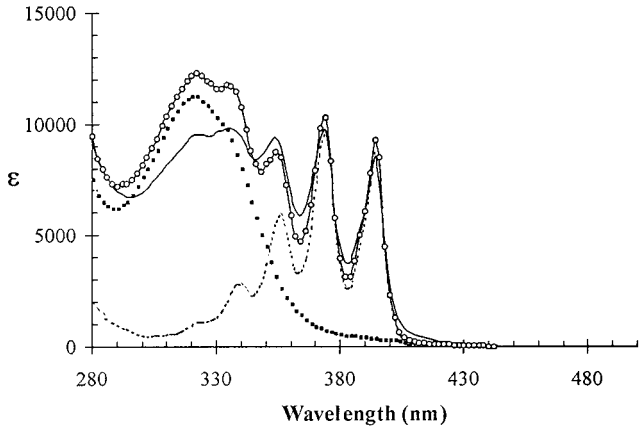

Figure 5. Comparison of the UV−vis spectrum of [Rh(anCH$_2$acac)(acac)$_2$] **5** (—) with the sum (−○−) of the UV−vis spectra of 9-methylanthracene (- - -) and [Rh(acac)$_3$] (■).

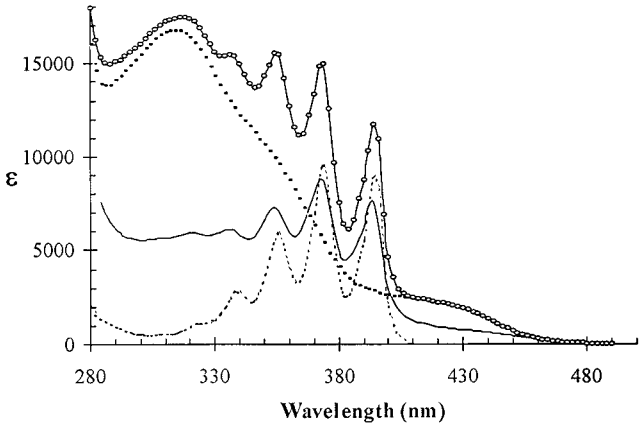

Figure 6. Comparison of the UV−vis spectrum of [Ir(anCH$_2$acac)(acac)$_2$] **6** (—) with the sum (−○−) of the UV−vis spectra of 9-methylanthracene (- - -) and [Ir(acac)$_3$] (■).

Table 4. Absorption and Fluorescence Data for 3-(9-Anthrylmethyl)pentane-2,4-dione **1** and Complexes **3**−**6** and Comparison with Those of 9-Methylanthracene[a]

	absorption		fluorescence[b]	
compound	λ_{max}	ϵ_{max}	λ_{max}	int_{max}
9-methylanthracene **7**	390	8900		100
3-(9-anthrylmethyl)pentane-2,4-dione **1**	394	9230	391	157
[Rh(acac)$_2$(anCOacac)] **3**	394	8650	390	0.3
[Ir(acac)$_2$(anCOacac)] **4**	392	7980	392	0.8
[Rh(acac)$_2$(anCH$_2$acac)] **5**	394	8560	392	0.9
[Ir(acac)$_2$(anCH$_2$acac)] **6**	394	7570	392	1.0

[a] All spectra were recorded in dichloromethane solution; λ are in nm; ϵ is given as M^{-1} cm^{-1}. [b] Excitation wavelength = 365 nm.

similar in all the compounds but is higher in **1** and in complexes **3**−**6** than in **7**. The rather significant reduction in the molar extinction coefficients observed on going from **1** and **7** to **3**−**6** is, at least in part, compensated by a marked broadening of the absorption bands. The fact that the oscillatory strength, the vibrational progression, and the absorption band position are similar in the spectra of **3**−**6** suggests that the same electronic transition is involved in all cases.

An indication of the existence of a strong interaction between the anthracene and the metal−β-ketoenolato moiety can be deduced by comparing the spectra of **3**−**6** with the

sum spectra obtained by adding the spectra of the various components (Figures 3−6). It is evident that the carbonyl spacer causes a strong reduction in the resolution of the vibrational progression, while the methylene spacer appears to insulate the structural subunits (compare Figures 3 and 4 with Figures 5 and 6). Furthermore, while the spectrum of [Rh(acac)$_3$] shows a weak tail at 400 nm ($\epsilon = 290$), the spectrum of [Ir(acac)$_3$] presents an intense band at the same wavelength ($\epsilon = 2610$) that causes a strong deformation of the absorption due to the anthrylic chromophore. A further indication of an interaction between the two moieties is given by the significant reduction of the absorption band at ca. 320 nm which is stronger in the model compounds, i.e., [Rh(acac)$_3$] and [Ir(acac)$_3$], than in the complexes **3**−**6**.

The fluorescence spectra of **3**−**6** and **1**, which were measured in dichloromethane at room temperature at the excitation wavelength of 365 nm, are quite similar to the spectrum of 9-methylanthracene **7** (Supporting Information). This suggests that, in all cases, the fluorescence emission is located on the anthrylic group. Indeed, no emission was observed for [Rh(acac)$_3$] and [Ir(acac)$_3$]. Although the spectra are similar, the emission intensity (Table 4) is drastically reduced in the complexes **3**−**6** compared with that of the reference compound **1**, the quenching being higher than 99% with only a small intensity increment passing from complexes **3** and **4**, which carry the carbonyl group as the spacer, to **5** and **6**, in which the two dyad components are connected by the methylene group.

The observed fluorescence quenching can be due to various mechanisms associated with an electron or energy transfer process, or with the increase of the rate of the intersystem crossing and/or of the internal conversion. Energy transfer depends on the overlap between the donor emission and the acceptor absorption spectra. No such correlation has been observed in the reported cases. On this basis, the occurrence of an energy transfer process as responsible for the anthryl fluorescence quenching can be considered unlikely, although the available data do not definitively rule out it. Indeed, owing to the significant modifications of the molecular geometry that are likely to occur in the electronic excited state, the absorption spectrum can change. Thus, the above correlation could exist after reorganization of the excited state. An increase of the intersystem crossing rate on going from anthracene to substituted anthracene derivatives would be observed only if, in the excited states, there is a strong electronic density on the metal. This can occur only if, after excitation, the molecular reorganization results in an electron transfer between the excited anthryl group and the metal−β-ketoenolato moiety. Finally, the presence of tails in the absorption spectra suggests that at least in some geometries the lowest excited states are strongly perturbed by the metal and are metal-centered. Obviously, this corresponds to a lowering of the energy of the lower excited states. The reduction of the energy gap between the first singlet excited state and the ground state is nevertheless not sufficient to increase the rate of internal conversion. Then, also this process appears to be unlikely. For all these reasons, we are strongly inclined to look at an intramolecular electron transfer process as the initial step responsible for the anthryl fluorescence quenching in the dyads **3**−**6**. This hypothesis is subject to the thermodynamic requirement that the resulting charge-separated state is exoergonic with respect to the anthracene-based excited state. In order to support this, a study of the electrochemical behavior of the dyads **3**−**6** was undertaken.

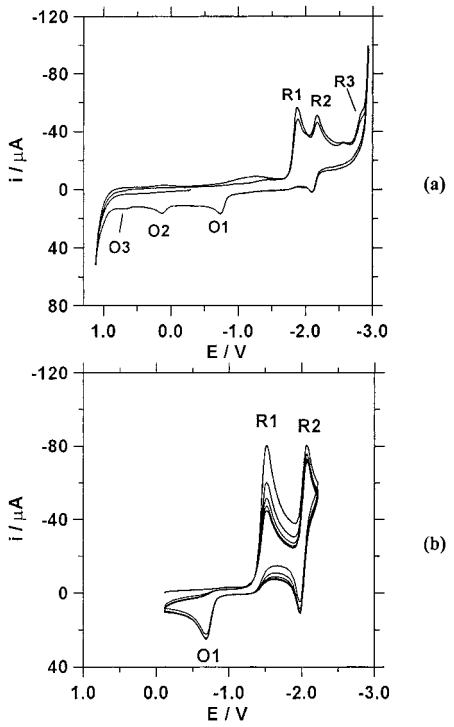

Figure 7. Multiple-scan cyclic voltammetric curves of a 1.0 mM THF solution of **5** (a), and of a 1.0 mM THF solution of **3** (b), both in the presence of TBAH (0.05 M). $T = 25$ °C; $v = 0.5$ V/s; working electrode: platinum.

Electrochemical Studies. Although the absorption spectra of compounds **3**−**6** show clearly that an electronic interaction exists between the two components, namely, the 9-substituted anthryl moiety and the metal−β-ketoenolate one, it cannot be ruled out that the localized redox orbital model,[39] i.e., the description of

the redox properties in terms of those of the two components, could be tentatively applied in studying the electrochemical behavior of **3**−**6**. Thus, in order to understand their CV behavior, [Rh(acac)$_3$] and [Ir(acac)$_3$] were first investigated as suitable model compounds (Supporting Information).

Figure 7a shows the CV curve obtained for [Rh(acac)$_2$(anCH_2acac)] **5**, whose electrochemical behavior is significantly reminiscent of that exhibited by [Rh(acac)$_3$].

In particular, as in the case of [Rh(acac)$_3$], the two-electron irreversible R1 peak and, in the reverse scan, the peaks O1−O3 are observed. According to the CV study of [Rh(acac)$_3$] (see Supporting Information), R1, O1, and O3 were attributed to a two-electron reduction and to two one-electron oxidations of the metal center, respectively, while O2 was due to the oxidation of free acetylacetonate anion ($acac^-$). The two additional one-electron-reduction peaks, R2 ($E_{1/2} = -2.14$

(39) Vlcek, A. A. *Coord. Chem. Rev.* **1982**, *43*, 39.

V; reversible) and R3 ($E_p = -2.85$ V; irreversible), are easily associated with the genesis of the radical anion and dianion of the anthryl group, respectively. Expectedly, the introduction of the anthrylic moiety causes significant changes in the CV behavior of the metal−β-ketoenolato moiety. R1 is largely shifted to less negative potentials ($E_p = -1.88$ V in **5** vs -2.21 V in [Rh(acac)$_3$]), and its half-width is also modified, the much narrower peak in **5** being now fully compatible with a Nernstian (fast) process. In the region of positive potentials, a one-electron-oxidation peak is observed (not shown in Figure 7a) having $E_{1/2} = 1.67$ V, attributed to the oxidation of the anthryl group.[40]

A similar CV behavior was observed in the case of [Rh(acac)$_2$(anCOacac)] **3** (Figure 7b). In particular, two anthryl-centered reductions, the first reversible ($E_{1/2} = -2.01$ V), were found to superimpose to the metal-centered two-electron-reduction/one-electron-reoxidation pattern due to the metal−β-ketoenolato moiety. As observed in the case of **5**, the R1 peak ($E_p = -1.51$ V) is anodically shifted with respect to [Rh(acac)$_3$] and the peak half-width approaches that of a Nernstian process. The anodic shift is, however, notably larger in **3** (770 mV) than in **5** (400 mV). Finally, an oxidation process ($E_{1/2} = 1.62$ V) is observed in the anodic region.

The effects observed on both the location and the shape of the metal-centered reduction R1 in **3** and **5**, when compared with that of [Rh(acac)$_3$], suggest the occurrence of a significant interaction between the anthryl moiety and the metal-containing component. The reversible and fast anthrylic unit reduction would play an important role in promoting the reduction of the kinetically impeded rhodium(III) center, by shuttling the incoming electrons to the metal core.[41] Such a process, which occurs intramolecularly, as indicated by the absence of any concentration effect on the CV pattern, would be driven by the very large overpotential for the rhodium(III) reduction [compare $E_p = -2.21$ V to $E_{1/2}$ (Rh^{III}/Rh^{II}) $= -0.68$ V, see Supporting Information]. In line with this hypothesis, the anticipation of the R1 peak is larger for **3**, having the carbonyl group as the spacer between the fluorophore and the metal-carrying component, than for **5**, which has the methylene group as the spacer.

Contrary to the rhodium derivatives, the CV investigation of the iridium derivatives is not indicative of any strong interaction between the two moieties, and the observed CV patterns result to be the superimposition of those of the separated models. The CV curve for [Ir(acac)$_2$(anCH$_2$acac)] **6** is reported in Figure 8. Three reduction peaks are observed in the cathodic scan. The R1 peak corresponds to a reversible one-electron reduction ($E_{1/2} = -1.97$ V), while R2 ($E_p = -2.60$) and R3 ($E_p = -2.90$) are irreversible.

By comparison with [Ir(acac)$_3$] and 9-methylanthracene, the first reduction is attributed to the 9-anthrylene moiety

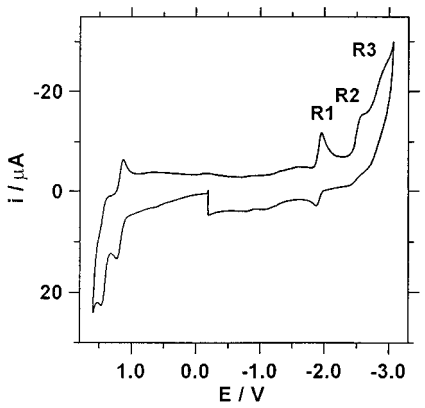

Figure 8. Cyclic voltammetric curve of a 1.0 mM THF solution of **6** in the presence of TBAH (0.05 M). $T = 25$ °C; $\nu = 0.5$ V/s; working electrode: platinum.

while the second reduction is attributed to the metal. The third process may correspond to the second reduction of either the anthryl group or the metal−β-ketoenolato moiety. Two oxidation peaks are observed in the anodic scan, the first reversible ($E_{1/2} = 1.16$ V, metal-centered), and the second ($E_p = 1.35$ V, anthryl unit-centered) partly irreversible.

A quite similar CV behavior was found for [Ir(acac)$_2$(anCOacac)] **4**. The same three-reduction pattern was observed, but, in this case, the first reduction, located at -1.66 V, is irreversible. This may indicate that in **4**, contrary to **3**, the reduced anthryl moiety may undergo a dimerization process, known to occur in position 10 in anthryl derivatives carrying electron-withdrawing groups at carbon atom 9.[42] Finally, **4** undergoes two oxidation processes in the anodic region with features similar to those observed for **6**. The two processes are located at $+1.20$ and $+1.45$ V and can be attributed to a metal-centered and to an anthracene-centered process, respectively.

In conclusion, the CV characterization of the dyads **3**−**6** led to the localization of the redox sites and to the evaluation of the standard potentials of either metal-centered or anthracene-centered redox processes. The data, which are gathered in Table 5, indicate clearly that, in the case of rhodium derivatives **3** and **5**, the metal center is expected to act as an electron acceptor; while, in the case of the iridium compounds **4** and **6**, the relatively easy metal oxidation makes the metal center either a potential donor or acceptor.

As previously anticipated, the occurrence of an intramolecular charge transfer process between the photoexcited anthrylic moiety and the metal−β-ketoenolato component may explain the strong quenching of emission in the dyads **3**−**6**. The driving force values for the photoinduced intramolecular electron transfer process, ΔG_{cs}, obtained within the Born model,[43] are given in Table 5. Even a rapid examination of these data shows clearly that the thermodynamic requirement for the occurrence of the photoinduced electron transfer is fulfilled in all the dyads **3**−**6**. In particular, as schematized in Figure 9, while in the case of the complexes **3**, **5**, and **6**,

(40) Inker, L. A.; Bard, A. J. *J. Am. Chem. Soc.* **1979**, *101*, 2316. Dietrich, M.; Heinze, J. *J. Am. Chem. Soc.* **1990**, *112*, 5142.

(41) Some similarity to the present system may be found, for instance, in the recently reported case of a 4-cyanobenzoate ester covalently linked to a nitroalkane group: Zi-Rong, Z.; Evans, D. H. *J. Am. Chem. Soc.* **1999**, *121*, 2941.

(42) Amatore, C.; Pinson, J.; Savèant, J. M. *J. Electroanal. Chem.* **1982**, *137*, 148.

Table 5. Redox Potential (Volts vs SCE, $T = 25$ °C) Parameters for Compounds **3**−**6**, [Rh(acac)$_3$], and [Ir(acac)$_3$][a] and Intramolecular Electron Transfer Free Energies

	oxidation		reduction		
compound	metal-centered	anthracene-centered	metal-centered	anthracene-centered	ΔG_{cs}/eV[f]
[Rh(acac)$_3$]	1.74[a,c]		−2.21;[c,d] (−0.68, −0.74)[e]		
[Ir(acac)$_3$]	1.20[b]		−2.60;[c] (−1.50);[e] −2.90[b]		
3		1.62[b]	−1.51[c,d]	−2.01;[c] −2.90	−1.10 (O); +0.35 (R)
4	1.20[b]	1.45[b]	−2.10;[c] −2.59[c]	−1.66[b]	−0.45 (O); −0.54 (R)
5		1.67[b]	−1.88[c,d]	−2.14;[c] −2.85[b]	−1.05 (O); +0.48 (R)
6	1.16[b]	1.35[c]	−2.60;[c] −2.90[c]	−1.97[b]	−0.55 (O); −0.23 (R)

[a] Reference 48, vs AgCl/Ag. [b] $E_{1/2}$. [c] E_p. [d] Two-electron peak. [e] $E_{1/2}$ obtained by digital simulation. [f] Calculated driving force for the photoinduced intramolecular charge transfer (either oxidative (O) or reductive (R) quenching, see text). In the calculation of ΔG_{cs}, the $E_{1/2}$ values of the respective [M(acac)$_3$] models, obtained from simulation, were used as the reduction potentials of metals. In the case of Rh compounds, the metal-centered oxidation potential reported in ref 48 for the model complex was used. A correction to the CS state energy of −0.2 eV was used for taking into account ion−solvent interactions.

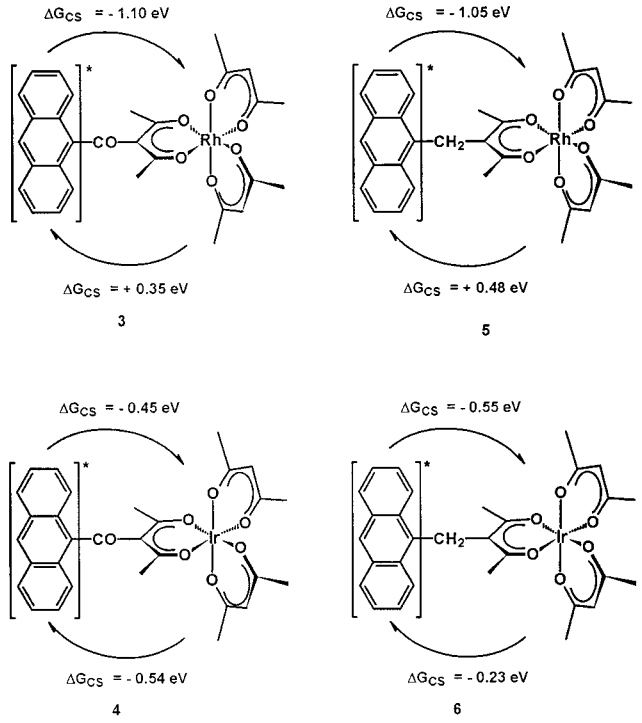

Figure 9. Representation of the intramolecular electron transfer for complexes **3**−**6** according to the evaluated energetics.

the transfer of one electron from the photoexcited anthryl group to the metal-carrying moiety is a thermodynamically favored process, in the case of **4**, the transfer of one electron from the metal−β-ketoenolato component to the anthryl group results to be slightly more favored.

EPR Studies. As discussed above, the fluorescence quenching observed for complexes **3**−**6** can be due to an intramolecular electron transfer. Accordingly, such a process should lead to the formation of a diradical which, in principle, could be detected by EPR spectroscopy. Thus, a number of experiments were carried out by irradiating dichloromethane solutions of complexes **3**−**6** with a xenon (150 W) high-pressure lamp directly into the cavity of an EPR spectrometer. Interestingly, we succeeded in obtaining a low-intensity EPR spectrum in all cases, at 190 K, but, unfortunately, no interpretation of the spectra could be done owing to their low resolution.

Instead, the EPR study of the reaction of the dyads **3**−**6** with reductants or oxidants led to much more interesting results which allowed a further insight into the electronic communication between the anthrylic moiety and the metal−β-ketoenolato component. However, we did not succeed in characterizing the products that resulted from the reaction of complexes **3**−**6** with several reductants.[44] Only in the case of the reaction of **3**−**6** with cobaltocene in CH_2Cl_2, a broad one-line EPR spectrum was observed, at temperatures ranging from −80° to 0° C. However, the absence of any hyperfine structure did not allow the identification of the detected radical species. Instead, the one-electron oxidation of **3**−**6** gave rise to the corresponding cation radicals, which were detected and characterized by EPR. Phenyliodine(III) bis(trifluoroacetate)[45] (PIFA) or tris(trifluoroacetate)thallium-(III) (TTFA) was used as oxidant, in 1,1,1,3,3,3-hexafluoropropan-2-ol (HFP). HFP is an ideal solvent for radical cations,[46] the only drawback being its relatively high melting point (−4 °C), which, however, was overcome by using a 1/1 (v/v) mixture of HFP and CH_2Cl_2. All the reactions were carried out, as previously described,[2b,c] by bringing the reagents into contact gradually, at −80 °C. Although both TTFA and PIFA resulted to be efficient one-electron oxidants, much more resolved spectra were obtained using TTFA. The experimental and simulated EPR spectra of the

(43) The driving force for the process may be calculated from the electrochemical and spectroscopic (emission) data by using the equation $-\Delta G_{cs} = E_{0-0} - (E^\circ_D - E^\circ_A) - \Delta G_s$, where E_{0-0} is the 0−0 energy of the anthracene-based excited state, estimated from the emission maximum in the model, 9-methylanthracene (3.2 eV), E°_D and E°_A are the standard potentials for the oxidation of the donor and the reduction of the acceptor, respectively, and, finally, ΔG_s is the correction term for the effects of ion−solvent interaction in the charge-separated (D^+-A^-) species, usually evaluated within the Born model. If the electrochemical and spectroscopic data refer to different media (as in the present study), ΔG_s also contains the correction for the polarity change on the standard potentials. (a) Weller, A. Z. *Phys. Chem.* **1982**, *93*, 1982. (b) Imahori, H.; Hagiwara, K.; Aoki, M.; Akiyama, T.; Taniguchi, S.; Okada, T.; Shirakawa, M.; Sakata, Y. *J. Am. Chem. Soc.* **1996**, *118*, 11771. (c) Van Dijk, S. I.; Groen, C. P.; Hartl, F.; Brouwer, A.; Verhoeven, J. W. *J. Am. Chem. Soc.* **1996**, *118*, 8452.

(44) Connelly, N. G.; Geiger, W. E. *Chem. Rev.* **1996**, *96*, 877.

(45) Kita, Y.; Tohma, H.; Inagaki, M.; Hatanaka, K.; Yakura, T. *Tetrahedron Lett.* **1991**, *32*, 4322.

(46) (a) Kita, Y.; Tohma, H.; Hatanaka, K.; Takada, T.; Fujita, S.; Mitoh, S.; Sakurai, H.; Oka, S. *J. Am. Chem. Soc.* **1994**, *116*, 3684. (b) Eberson, L.; Hartshorn, M. P.; Persson, O. *J. Chem. Soc., Perkin Trans. 2* **1995**, 1735. (c) Eberson, L.; Hartshorn, M. P.; Persson, O.; Radner, F. *Chem. Commun.* **1996**, 2105.

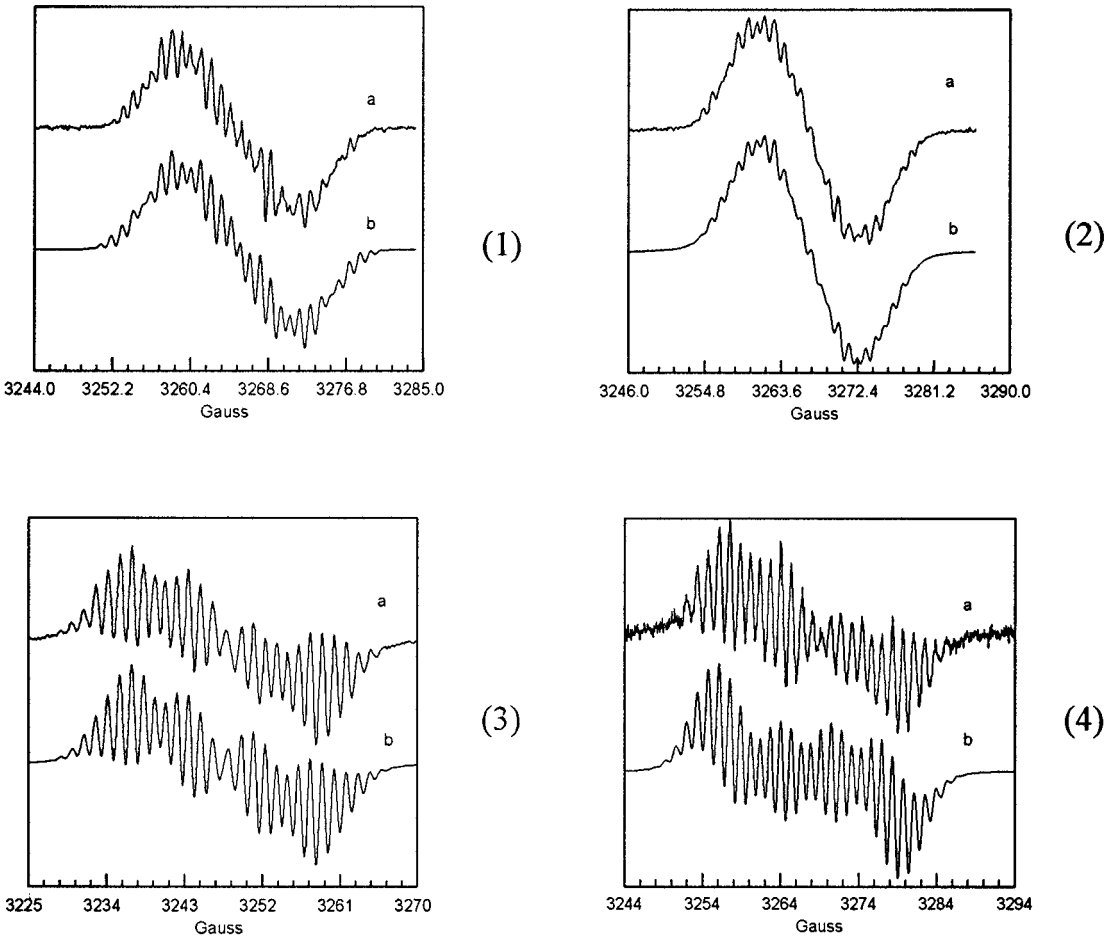

Figure 10. Experimental (a) and simulated (b) first-derivative X-band EPR spectrum of (1) $[Rh(acac)_2(anCOacac)]^+$ $\mathbf{3}^+$, (2) $[Ir(acac)_2(anCOacac)]^+$ $\mathbf{4}^+$, (3) $[Rh(acac)_2(anCH_2acac)]^+$ $\mathbf{5}^+$, and (4) $[Ir(acac)_2(anCH_2acac)]^+$ $\mathbf{6}^+$.

Table 6. EPR Data for the Cation Radicals $\mathbf{3}^+-\mathbf{6}^+$

cation radical	T (K)	ΔH_{pp} (G)	hyperfine coupling constant (G) (nucleus)	g_{iso}
$[Rh(acac)_2(anCOacac)]^+$ $\mathbf{3}^+$	253	0.33	6.25 (1H);[a] 0.26 (2H); 2.41 (2H); 2.81 (2H); 3.08 (2H); 1.00 (6H); 1.37 (Rh)	2.0055
$[Ir(acac)_2(anCOacac)]^+$ $\mathbf{4}^+$	263	0.33	5.50 (1H);[a] 0.95 (2H); 3.90 (2H); 1.83 (2H); 2.09 (2H); 1.34 (6H)	2.0055
$[Rh(acac)_2(anCH_2acac)]^+$ $\mathbf{5}^+$	243	90%: 0.63	90%: 7.37 (1H);[a] 1.47 (2 H); 2.94 (2H); 1.35 (2H); 1.21 (2H); 1.29 (6H); 6.58 (2H)	90%: 2.0177
		10%: 1.01	10%: 17.32 (1H);[b] 1.48 (6H);[c] 1.40 (2H)	10%: 2.0055
$[Ir(acac)_2(anCH_2acac)]^+$ $\mathbf{6}^+$ [d]	243	0.54	2.88 (1H);[a] 1.33 (2H); 0.99 (2H); 1.36 (2H); 1.38 (2H); 1.63 (2H); 6.45 (Ir)	2.0055

[a] According to the literature,[47] this hyperfine splitting constant is attributed to the coupling of the unpaired electron with the proton on carbon atom 10 of the anthrylic moiety. [b] According to the literature,[2] this hyperfine splitting constant is attributed to the coupling of the unpaired electron with the intercarbonylic proton of one pentane-2,4-dionate ligand. [c] According to the literature,[2] this hyperfine splitting constant is attributed to the coupling of the unpaired electron with six magnetically equivalent protons of two methyl groups of the pentane-2,4-dionate ligand. [d] In this case, owing to the low signal-to-noise ratio, the spectrum simulation did not allow us to state unambiguously whether other EPR signals were present.

cation radicals $\mathbf{3}^+-\mathbf{6}^+$ are shown in Figure 10, while the hyperfine coupling constants and line widths are reported in Table 6.

In all cases an extended spin delocalization is observed: the unpaired electron interacts with all the anthrylic protons, the methyl protons of the anthryl-substituted β-ketoenolate, and the methylene protons of the spacer. Moreover, in the radical cation $\mathbf{3}^+$ and $\mathbf{6}^+$, spin delocalization over the metal is also observed, the interaction of the unpaired electron with the iridium nucleus being higher than that with the rhodium nucleus. The EPR spectrum of the radical cation $\mathbf{5}^+$ has been computer simulated as the superimposition of two radical species which are present in 90% and 10%, respectively. The main species is associated with a radical cation whose unpaired electron is delocalized over the anthracene moiety, the spacer, and the two methyl groups of the anthryl-substituted β-ketoenolate ligand, whereas the other species shows a spin delocalization over the intercarbonylic proton of a pentane-2,4-dionate ligand, over the two methyl groups of the same ligand and over other two protons. A semiempirical calculation of the spin density distribution of the radical cation $\mathbf{5}^+$ shows that the spin delocalization is markedly influenced by the conformation of the anthryl-methyl group, as shown in Figure 11.

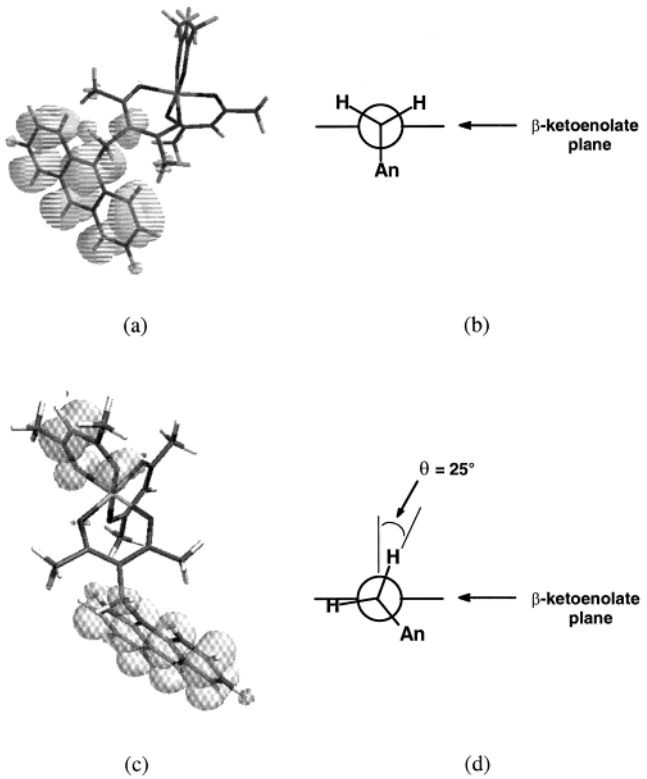

Figure 11. Calculated (Spartan 5.1.3) spin density distribution surface (0.001 e/au^3) for the radical cation $\mathbf{5}^+$ (a and c) and Newman projections at the methylenic carbon atom (b and d).

Figure 11a shows that when the anthracene is oriented as reported in Figure 11b, the unpaired electron delocalizes almost totally over the anthrylmethyl-substituted β-ketoenolate ligand. Interestingly, the same electron-spin distribution is observed for the most abundant radical species generated by oxidation of **5**. By rotation of the anthrylic group of about $\pm 25°$ around the intercarbonylic C$-$CH$_2$ bond (Figure 11d), a new conformer is obtained whose spin delocalization interests mainly the anthracene moiety and one of the unsubstituted acetylacetonate ligands (Figure 11c). As before, this spin distribution is in perfect agreement with the one observed for the radical cation obtained as minor product from the oxidation of **5**, although the spin distribution over the anthracene skeleton is probably too low to be observed. The semiempirical calculation of the spin density distribution for the radical cations $\mathbf{3}^+$, $\mathbf{4}^+$, and $\mathbf{6}^+$ leads to analogous results (Figure 12).

In conclusion, the radical cations $\mathbf{3}^+-\mathbf{6}^+$ show a high spin delocalization which is markedly influenced by the conformation assumed by the anthrylmethyl group. In other words, a large electronic interaction may take place between the subunits constituting the dyads **3**$-$**6**, i.e., the metal$-\beta$-ketoenolato core and the anthryl group, depending upon the molecular conformation. As a final comment, it must be pointed out that although the employed spacers, i.e., the methylene and the carbonyl, have a strongly different chemical nature, nevertheless they allow an efficient electronic communication between the two subunits.

The possibility to get a further insight into the electronic properties of the above cation radicals was explored through

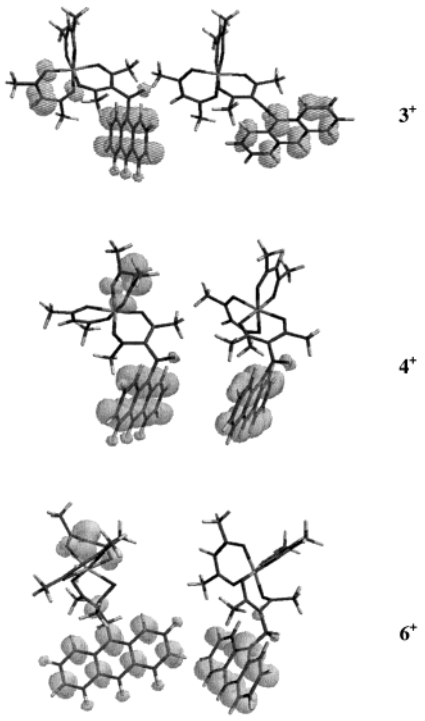

Figure 12. Calculated (Spartan 5.1.3) spin density distribution surface (0.001 e/au^3) for two different anthrylmethyl conformations of the radical cations [Rh(acac)$_2$(anCOacac)]$^+$ $\mathbf{3}^+$, [Ir(acac)$_2$(anCOacac)]$^+$ $\mathbf{4}^+$, and [Ir(acac)$_2$(anCH$_2$acac)]$^+$ $\mathbf{6}^+$.

the DFT calculation of the spin density distribution of the rhodium derivatives $\mathbf{3}^+$ and $\mathbf{5}^+$ by using the Spartan 5.1.3. program (model LSDA/pBP86/DN**) (Figure 13).[49]

The resulting spin density distribution shows clearly that, in the optimized geometry, the unpaired electron delocalizes over the whole molecular skeleton, including all the β-ketoenolato rings, the rhodium center, and the 9-anthryl moiety. The discrepancy between the experimental and theoretical data is, in our opinion, only apparent since, as discussed above, the spin density distribution in the cation radicals $\mathbf{3}^+-\mathbf{6}^+$ is extremely sensitive to even small conformational variations of the anthrylmethyl fragment. It is thus not surprising that the DFT calculations of the spin density distribution in $\mathbf{3}^+$ and $\mathbf{5}^+$ converge to the molecular geometry shown in Figure 13, which gives rise to the energy minimum implying high spin delocalization. A possible conclusive consideration is then that one should look at the detected cation radicals as transient species which decay before they have the time to reach the most energetically favored geometry.

Concluding Remarks

9-Anthrylmethyl- and 9-anthroyl-substituted heteroleptic β-ketoenolato derivatives of rhodium(III) and iridium(III), **3**$-$**6**, can be easily prepared by alkylation or acylation of the corresponding tris-acetylacetonates under Friedel$-$Crafts

(47) Carrington, A.; McLachlan, A. D. *Introduction to Magnetic Resonance*; Harper & Row: New York, Evanston and London, and John Weatherhill Inc.: Tokyo, 1975.
(48) Tocher, J. H.; Fackler, J. P., Jr. *Inorg. Chim. Acta* **1985**, *102*, 211.
(49) Spartan Version 5.1.3, Wavefunction, Inc., 18401 Von Karman Avenue, Suite 370, Irvine, CA 92612.

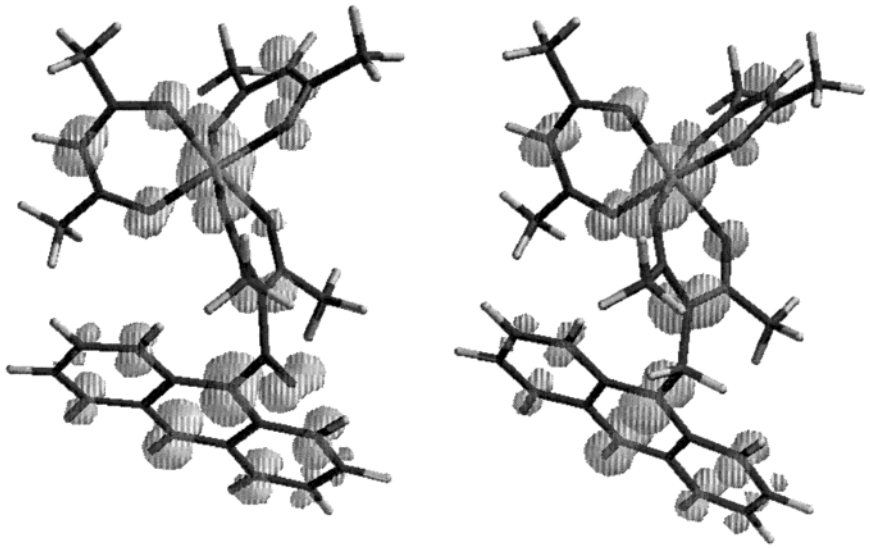

Figure 13. DFT calculated (Spartan 5.1.3) spin density surface (0.002 e/au^3) of the radical cations $[Rh(acac)_2(anCOacac)]^+$ $\mathbf{3}^+$ (left) and $[Rh(acac)_2(anCH_2acac)]^+$ $\mathbf{5}^+$ (right).

conditions. All the investigated properties of the dyads **3**−**6** substantiate the existence of a significant electronic interaction between the subunits, i.e., the metal−β-ketoenolato core and the anthryl group that constitute the dyads. Such an interaction results to be higher when the subunits are connected through the carbonyl group. While 3-(9-anthrylmethyl)pentane-2,4-dione, $anCH_2acacH$, is an efficient light-emitting molecule, the fluorescence of the anthryl group is strongly quenched in **3**−**6** probably because of the occurrence of an electron transfer between the photoexcited anthrylic subunit and the β-ketoenolato−metal moiety. In support of this is the free energy change associated with such an electron transfer. The EPR characterization of the cation radicals of **3**−**6** shows that the spin distribution within the molecular skeleton depends strongly on the conformation assumed by the 9-anthrylmethyl and 9-anthroyl moieties. This demonstrates that the electronic communication between the components of dyads **3**−**6** depends not only on their skeletal structure but also on the molecular conformation. Since this varies markedly with temperature, it is expected that some of the electronic properties associated with **3**−**6** as a whole could significantly depend on temperature.

In conclusion, the present investigation shows that the dyads **3**−**6** have a lot of interesting chemical and photophysical peculiarities. In this connection, an important point that should univocally be verified is the formation of charge-separated species as a consequence of the suggested intramolecular electron transfer between the photoexcited anthryl group and the β-ketoenolato−metal moiety, which is responsible for the quenching of the anthrylic fluorescence. Such charged species are expected to exhibit very different electronic and optical properties if compared with those of the starting neutral complexes **3**−**6**. These features could well be used to project new molecular devices capable to give an electric or an optic response as a consequence of light absorption. Moreover, owing to the electronic communication lying between the subunits of the dyads **3**−**6**, it can be conjectured that high-molecular-weight compounds, constituted by alternating anthryl and metal−β-ketoenolato moieties, interconnected through an appropriate spacer, could behave as solid conductor or semiconductor, under photochemical or chemical activation conditions. Work is now in progress aimed to verify some of these points.

Acknowledgment. We thank Dr. A. Raffaelli (Centro per lo Studio delle Macromolecole Stereoordinate ed Otticamente Attive, CNR, Pisa, Italy) for obtaining the ion spray mass spectra of compounds **3**−**6**. Financial support from MURST (Rome, Italy) and from the University of Bologna (Funds for Selected Research Topics) is kindly acknowledged.

Supporting Information Available: X-ray crystallographic files in CIF format for the structure determinations of **1** and **3**; the fluorescence spectra of compounds **1**, **3**−**6**, and **7**; details of the study of the electrochemical behavior of $[Rh(acac)_3]$ and $[Ir(acac)_3]$. This material is available free of charge via the Internet at http://pubs.acs.org.

IC010698X